

A COMPARATIVE STUDY OF COMPUTATIONAL
METHODS IN COSMIC GAS DYNAMICS

(an extension)

Catherine Campbell-Grant

September 2004

Supervisor: Dr.P.K.Sweby

CONTENTS PAGE

Summary	3
Introduction	3
The Problem	4
Background Physics	9
The Methods	16
How we apply the methods	16
Testing the Methods	19
MacCormack's method	20
Second-order flux-splitting method	23
Approximate Riemann Solvers	27
Roe's Scheme	29
Roe's Scheme with flux limiters	33
Roe's Scheme with the source term decomposed and flux limiters applied	41
The HLL Scheme and the HLL Scheme with flux limiter applied	49
The HLLC Scheme and the HLLC Scheme with flux limiter applied	60
Calculated errors in the smooth zone	70
Results	72
Conclusions and Recommendations	74
Appendix	75
Acknowledgements	84
References	84

A COMPARATIVE STUDY OF COMPUTATIONAL METHODS IN COSMIC GAS DYNAMICS (an extension)

SUMMARY

We compare how well some computational methods model a representative astrophysical flow problem. This is an extension of a paper written in 1981.

We use the two best methods in the paper plus : Roe's method; Roe's method with flux limiters applied; Roe's method with the source term decomposed and flux limiters applied; the HLL-method; the HLL-method with flux limiter applied; the HLLC-method; the HLLC-method with flux limiter applied.

INTRODUCTION

In a paper entitled 'A Comparative Study of Computational Methods in Cosmic Gas Dynamics' written in 1981, Van Albada, Van Leer, and Roberts, Jr. [12] compared some computational methods on a representative astrophysical flow problem in order to acquaint astronomers with the virtues and failings of typical numerical methods.

The methods they used were the Beam scheme, Godunov's method, second-order flux-splitting method, MacCormack's method and the flux corrected transport method of Boris and Book. Since 1981 there has been substantial progress in computational methods. This work therefore extends the paper to explore new methods which may be an improvement on the methods previously studied.

THE PROBLEM (as stated in the previous paper [12])

Our test problem is a simple, one-dimensional model of the gas flow in a spiral galaxy.

The generally accepted theory for the coherent, large-scale spiral patterns observed in many galaxies is the density wave theory of Lin and Shu (1964, 1966) [6, 7].

The density wave theory states that the spiral-arm pattern is caused by a spiral density wave. This is a supersonic compression wave of increased density that moves through the stars and gas in the galaxy.

The wave rotates more slowly than the actual material causing the density of the material to build up. A shock wave builds up and possible outcomes are star formation and increased collisions of giant molecular clouds.

Roberts wrote a paper in 1969 [8] in which he used one-dimensional, steady state gas equations which included a forcing term due to the spiral field of stars. He showed how a mild stellar structure can induce shock waves in the gas and how this effects the observed features of the spiral structure. The actual evolution of the flows was studied by Woodward in 1975 [15] where he used a simplified time-dependent version of Roberts' equations.

We use Woodward's equations and a set of his parameter values here.

The nonlinear response of the gas to an imposed spiral gravitational field has several distinguishing characteristics of astrophysical flows (i.e. a major role is played by source terms, strong shocks are apt to develop and rotational effects are significant).

When we explore the numerical methods we note that:

1. Source terms can lead to unexpected behaviour in numerical methods which are usually analysed and tested in the absence of such terms.
2. Strong shocks demand reliability.
3. The proper treatment of angular momentum requires accuracy.

Often methods cope well with the shock only by artificially redistributing the angular momentum. This can be a serious problem when we are investigating the dynamics of the gas.

The equations in an inertial frame for an isothermal gas are:

$$\frac{\partial Q}{\partial t} + \nabla \cdot (Qq) = 0, \quad (1)$$

$$\frac{\partial q}{\partial t} + q \cdot \nabla q = \frac{-c}{Q} \nabla Q - \nabla \Phi, \quad (2)$$

where Q is the density, q is the velocity, c is the (constant) sound speed and Φ is the gravitational potential.

We can assume that the flow is isothermal since the gas cools by radiative processes much quicker than it takes for any dynamical processes to take place.

Without spiral forcing the gas flows round in a circle and has an angular velocity of $\Omega(r)$ at radius r . A steady spiral field with small pitch angle α is assumed to rotate with pattern speed Ω_p . We will use a coordinate system which rotates at this speed

and is aligned with the equipotential contours of the spiral. We denote the coordinates parallel and perpendicular to the equipotential contours by \mathbf{x} and \mathbf{h} respectively.

The velocity components in this system are written as:

$$v = q_{\mathbf{x}}, \quad (3)$$

$$u = q_{\mathbf{h}}.$$

We take the spiral pattern to be tightly wound (so that $\mathbf{a} \ll 1$) and the equilibrium velocities to be approximately:

$$v_0 = r(\Omega - \Omega_p), \quad (4)$$

$$u_0 = \mathbf{a}r(\Omega - \Omega_p).$$

In this approximation derivatives with respect to \mathbf{h} (normal to the spiral arms) are retained, but derivatives with respect to \mathbf{x} (along the spiral arms) are discarded. For a two-armed spiral the resulting equations can be written as the system of conservation laws:

$$\frac{\partial U}{\partial t} + \frac{\partial F}{\partial \mathbf{h}} = \mathbf{H}, \quad (5)$$

where the vector of conserved quantities is

$$U = \begin{pmatrix} Q \\ Qu \\ Qv \end{pmatrix}, \quad (6)$$

the vector of fluxes is

$$F = \begin{pmatrix} Qu \\ Q(u^2 + c^2) \\ Quv \end{pmatrix}, \quad (7)$$

and the vector of source terms is

$$H = \begin{pmatrix} 0 \\ 2\Omega(v - v_0)Q + \frac{2}{ar}QA \sin \mathbf{h} \\ -\frac{k^2}{2\Omega}(u - u_0)Q \end{pmatrix}. \quad (8)$$

The spiral phase \mathbf{h} is defined by

$$\mathbf{h} = \frac{2\mathbf{h}}{ar} \quad (9)$$

and the epicyclic frequency \mathbf{k} by

$$\mathbf{k}^2 = \frac{2\Omega}{r} \frac{d}{dr}(r^2\Omega). \quad (10)$$

In this approximation the flow is periodic. In terms of the spiral phase the periodicity condition reads

$$U(\mathbf{h}, t) = U(\mathbf{h} + 2\mathbf{p}, t). \quad (11)$$

In these equations $\frac{2}{ar}QA \sin \mathbf{h}$ is a driving term. This arises from the assumed

gravitational field of the stellar component. While $2\Omega(v - v_0)Q$ is called the inertial

term and is related to gravitational, centrifugal and Coriolis forces.

The parameters that we shall assume in our test problem that are thought to be appropriate to the neighbourhood of the Sun in our galaxy are:

$$\begin{aligned} \Omega &= 25 \text{ km s}^{-1}/\text{kpc} & \Omega_p &= 13.5 \text{ km s}^{-1}/\text{kpc} \\ k &= 31.3 \text{ km s}^{-1}/\text{kpc} & c &= 8.56 \text{ km s}^{-1} \\ r &= 10 \text{ kpc} & a &\approx 0.11667 \end{aligned}$$

We choose $A=72.92 \text{ (km s}^{-1})^2$ for the amplitude so that the amplitude of the spiral force is two percent of the equilibrium force $r\Omega^2$.

In the steady state (5) becomes:

$$\begin{aligned} \frac{du}{d\mathbf{h}} &= \frac{u}{u^2 - c^2} \left[2\Omega(v - v_0) + \frac{2A}{ar} \sin \frac{2\mathbf{h}}{ar} \right], \\ \frac{dv}{d\mathbf{h}} &= \frac{-k^2}{2\Omega} \left(\frac{u - u_0}{u} \right) \end{aligned} \tag{12}$$

In the case that we study there is a shock at $\mathbf{h} = 131.68^\circ$ and the flow becomes supersonic with a sonic point at $\mathbf{h} = 155.53^\circ$. In Robert's paper 1969 [8] he shows a method to solve (12) in conjunction with (11). In this flow there is a rapid decompression after the shock and a secondary structure near $\mathbf{h} = 270^\circ$ caused by resonance effects. The time dependent version of this is modelled best by numerical methods that are able to deal with the shock while also resolving the rest of the structure well.

BACKGROUND PHYSICS

MATERIAL FROM ROBERTS, 1969 [8]

When we look at the overall structure of galaxies we often see a spiral structure occurring. Over the years many scientists have tried to explain what causes this grand design to happen. One theory associates each spiral arm with a specific body of matter throughout the arms evolution however this causes a winding problem when we consider differential rotation. Another suggested theory is the density wave theory. Originally this was studied by B.Linblad by considering the properties of individual stellar orbits; however this was not very convincing. Later P.O. Linblad studied the stellar collective modes and had more success. After his studies there was still a need to understand how such a structure could stay quasi-stationary but this was soon solved by an asymptotic theory developed by Lin and Shu.

In galaxies we see the young stellar associations and brilliant HII Regions appearing in chains and spiral arcs within the spiral structure. They lie along the inner sides of the observed gaseous spiral arms. Therefore we see that star formation takes place over an even narrower region than the total spiral arm width. Considering the short amount of time the gas stays in the spiral arm and the fact that in the linear theory the gas concentration in a density wave extends over a broad region we would not expect to find such narrow strips of newly born stars. To explain these strips we therefore turn to the existence of 'galactic shocks'. In fact over time we might expect self-sustained density waves to turn into shocks.

The factors that effect the gas dynamics in this system are:

1. The inertial force associated with the rotation of the disc.
2. The smoothed gravitational force of the system as a whole.
3. Gaseous 'pressure' associated with turbulence in the interstellar medium and the hydromagnetic forces (due to magnetic fields embedded in the interstellar medium)
4. Primary sources of the turbulent energy for the gas:
 - cosmic rays
 - supernova explosions
 - stellar radiation
5. The effect of dissipation of turbulence by collisions of gas clouds (the primary sink of turbulent energy for the gas).

We visualise each gas streamtube to have a uniform mean turbulent dispersion speed.

The gas flow along each streamtube being isothermal at a uniform mean equivalent turbulent temperature.

Now, we know that the majority of the stars and gas are within a layer which is from one fiftieth to one hundredth of the diameter of the galactic disc. We can therefore 'squeeze' our problem so that it all takes place over an infinitely thin sheet. We translate our physical variables into this setting by integrating over the layer's thickness and taking the mean values. In this problem we shall mainly be concerned with the response of the gas to an imposed background spiral gravitational field.

To resolve this problem we need to look at the fundamental equations of motion for gas flow about the circular disc. Our base state of motion is the Schmidt model (our galaxy) in which there is an equilibrium state of purely circular gas flow. This equilibrium is caused by the total smoothed central gravitational force field exactly balancing the inertial force associated with the rotation of the disc as a whole. Our coordinate system for this model consists of the radius out from the centre and the angle we have rotated around our circle. Building on this model we are able to construct a perturbed state which superposes a two-armed spiral field on top of the Schmidt model. Here we shift the coordinate system to be the one we use in this paper. The coordinates are fixed in a Ω_p -rotating system and are parallel and perpendicular to the spiral equipotential curves.

In the asymptotic theory the perturbation quantities to the first order vary only along the direction normal to the contours of constant phase. This sort of approximation is first thought of by noticing that the imposed spiral potential is oscillatory as cosine normal to the contours of constant phase and only slowly varying parallel to them.

When we are using the non-linear gas flow equations we are primarily interested in solutions which satisfy the following:

1. They permit the gas to pass through two periodically located shock waves which lie coincident with spiral equipotential curves in the disc.
2. They describe the gas flow along a narrow, nearly concentric streamtube band about the galactic centre, and the streamtube should repeat itself through every half revolution of the gas flow about the disk.

3. They ensure closure of the gas streamtube so that no net radial transfer of mass, momentum, or energy takes place across the streamtube.

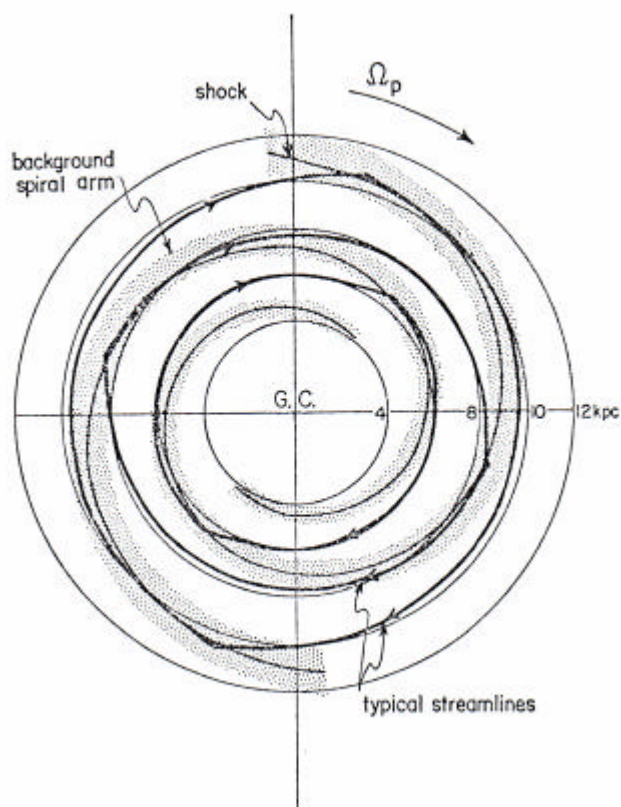
This provides a solution of gas flow in a closed, nearly concentric and twice periodic streamtube band through two periodically located shock waves (otherwise known as an STS solution).

The variables that determine the nature of the STS solution are:

- i) the angle of inclination of a spiral arm to the circumferential direction;
- ii) the angular speed of the spiral pattern;
- iii) the amplitude of the spiral gravitational field taken as a fixed fraction of the smoothed axisymmetric gravitational field;
- iv) the average radius of the streamtube;
- v) the mean turbulent dispersion speed of the gas along the streamtube.

Once the three STS conditions have been satisfied and we have specified the values for all of the above mentioned variables the shock location with respect to the background spiral arm is determined.

The shape of our graphs in the rest of this paper are illustrated in the diagram below. From this diagram we can see that the density suddenly increases (shock appears) at the same point that the velocity normal to the contours of constant phase decreases and the velocity parallel to them increases.



The outer bound of the spiral pattern is dependent on the number of arms in the spiral design and the spiral gravitational field taken as a fixed fraction of the smoothed axisymmetric gravitational field.

If we now try to visualise how a galaxy will look we see that:

1. The background distribution of moderately old stars will not be seen.
2. We will notice the gaseous spiral arms.
3. The newly luminous stars and brilliant HII regions will stand out.

Therefore translating our graphs to the observable spiral features of the galactic structure we see that the point of phase from our shock on the density graph to the point at which the density falls below unity is the region in which our spiral arm lies.

Now, if an upper bound of thirty million years is taken for the formation and evolution of relatively massive stars we see that the possible locations for the regions of new stars and their associated HII Regions are on the inner side of the observable HI spiral arms. They stretch from the shock to approximately the centre of the arm and so on the graph are contained in the left most part of the section we specified above.

MATERIAL FROM WOODWARD, 1974 [15]

Most of the time-dependent results presented in Woodward's paper use the isothermal equation of state. The isothermal flow equations scale with the density and so the average density chosen is unimportant. By solving these equations he was able to gain insight into how and why the shock forms. Looking at his equations it was seen that time-reversal symmetry and so shockless steady flow solutions were possible. However for sufficiently large wave amplitudes the symmetry is broken when irreversible processes occur in the gas and a shock is formed. The shock's development takes place as follows:

1. Initially the steepening is a result of the tendency of the gas in the wave crests to flow more rapidly than the gas in the wave troughs in the direction of the wave propagation. This is called convective steepening.
2. Later there is an increase in the effectiveness of pressure forces in opposing convective steepening near the wave crests relative to the wave troughs.
3. The final stage of the steepening is caused by inertial and gravitational forces.

When a resonance condition is met (i.e. the spiral driving potential rotates at an angular frequency equal to that of a free mode of oscillation of the system) then the second harmonic component of the density wave form can grow unusually large.

If the symmetry is broken by numerical viscosity, it is natural that the resonance should be altered or diminished, if not eliminated. Resonant conditions for higher harmonics can be found if they are not damped out by the numerical viscosity.

Harmonic resonance may provide an explanation for secondary spiral features such as spiral arm spurs, branches, or feathers.

THE METHODS

The schemes that we shall study are:

- a) MacCormack's method (studied in the previous paper [12])
- b) Second-order flux splitting method (studied in the previous paper [12])
- c) Roe's scheme
- d) Roe's scheme with flux limiters
- e) Roe's scheme with flux limiters and the source term decomposed
- f) The HLL scheme
- g) The HLL scheme with the minmod limiter applied
- h) The HLLC scheme
- i) The HLLC scheme with the superbee limiter applied to the contact field and minmod applied elsewhere

We choose to study (a) and (b) from the previous paper as these suited the problem the best from the last investigation. We then go on to investigate the methods (c), (d), (e), (f), (g), (h) and (i) to examine whether they produce even better results.

HOW WE APPLY THE METHODS

Firstly, the definition of some of the notation that we shall use here is as follows:

U_i^n is the approximate value of U at (\mathbf{h}_i, t_n) ,

$F_i^n = F(U_i^n)$ and

$H_i^n = H(U_i^n, \mathbf{h}_i)$ (or $H(U_i^n, \mathbf{h}_i, \Delta t)$).

This is when the subscript i denotes the value at the spatial point $i\Delta\mathbf{h}$ (with

$\Delta\mathbf{h} = \frac{\mathbf{par}}{N}$ or equivalently $\Delta\mathbf{h} = \frac{2\mathbf{p}}{N}$) and the superscript n denotes the value at

temporal point $n\Delta t$.

The schemes can be written in the form

$$\frac{U_i^{n+1} - U_i^n}{\Delta t} + \frac{\mathbf{f}_{i+\frac{1}{2}}^v - \mathbf{f}_{i-\frac{1}{2}}^v}{\Delta\mathbf{h}} = H_i^{n+\frac{1}{2}} \quad (13)$$

with $v = n$ or $v = n + (1/2)$. This approximates (5) in the so-called ‘‘conservation form’’ and is obtained from a discretised version of the partial differential equations.

The numerical flux vector

$$\mathbf{f}_{i+\frac{1}{2}}^v \equiv \mathbf{f}(U_{i-k+1}^n, \mathbf{K}, U_{i+k}^n) \quad (14)$$

is a function of $2k$ initial values. At a certain time step it is taken to be our F at $\mathbf{h}_{i+\frac{1}{2}}$

and is determined by the particular numerical method we are using.

In applying our numerical methods we divide our spatial region $(0, \mathbf{par})$ into N equal zones. The edge of the zones are at $i\Delta\mathbf{h}$ where $i = 0, \Lambda, N$. Using (13) we can progress our values from t_n to t_{n+1} .

The methods are usually stable under the CFL condition, which states that the largest radial wave or material speed in a cell must not exceed the numerical signal speed.

In most of the methods that we study in this paper we accounted for the source terms in separate steps.

First, we approximated

$$\frac{\partial U}{\partial t} = H, \quad (15)$$

over a half time-step, then continued by approximating

$$\frac{\partial U}{\partial t} + \frac{\partial F}{\partial \mathbf{h}} = 0, \quad (16)$$

over a whole time-step, finally completing this by approximating (15) again over a half time-step.

This method has the advantage that (15) can be solved analytically for the current problem. The solution is as follows:

$$Q(t_n + \mathbf{t}, \mathbf{h}_i) = Q_i^n,$$

$$u(t_n + \mathbf{t}, \mathbf{h}_i) - u_0 = (u_i^n - u_0) \cos(\mathbf{k}\mathbf{t}) + \frac{2\Omega}{\mathbf{k}} (v_i^n - v_0 + \frac{A}{ar\Omega} \sin \mathbf{h}) \sin(\mathbf{k}\mathbf{t}), \quad (17)$$

$$v(t_n + \mathbf{t}, \mathbf{h}_i) - v_0 = \frac{-A}{ar\Omega} \sin \mathbf{h} + (v_i^n - v_0 + \frac{A}{ar\Omega} \sin \mathbf{h}) \cos(\mathbf{k}\mathbf{t}) - \frac{\mathbf{k}}{2\Omega} (u_i^n - u_0) \sin(\mathbf{k}\mathbf{t}).$$

The use of such an accurate solution proved essential for maintaining stability of very long runs (over 2000 time-steps).

TESTING THE METHODS (as in the previous paper [12])

TEST ONE

Since the exact solution is only known reliably at the steady state limit we cannot compare the methods on how well they model the time evolution of the flow. We therefore choose to test how accurately the methods produce the steady state. Also, due to reasons stated in the previous paper we choose to take the exact steady state solution as the initial value distribution and compare how well each of the methods preserve it.

Note that the values taken at the start U_i^0 are zone-averaged values of the exact solution in order to be consistent with the data representation of the methods.

During this investigation we found that although the exact solution is known it is not readily available. We therefore turned to the last paper for assistance in this matter.

TEST TWO

We will only apply this test to the methods which performed the best in test one.

Here we take uniform initial values $(Q, u, v)_i^0 = (1, u_0, v_0)$ to determine the “robustness” of the methods.

In test one we use 64 spatial zones and progress the values by 1200 time-steps from the exact steady-state with a constant time-step corresponding initially to a global Courant number of 0.5.

In test two we shall progress the values by 2400 time-steps.

a) MACCORMACK'S METHOD (as in the previous paper [12])

This was developed by MacCormack in 1969 and has been widely used in aerodynamics.

In this method one-sided differencing is used twice, first to one side and then to the other. In implementation we can either apply the one-sided differences in the same order repeatedly or alternate them to obtain a more symmetric system. We will use the latter type of method here.

It is a method that is formally second order accurate in both space and time and that does not require you to approximate the Jacobian matrix or its eigenstructure.

On even time steps we will apply a forward predictor step which will determine the provisional values at t_{n+1} ,

$$\bar{U}_i^{n+1} = U_i^n - \frac{\Delta t}{\Delta \mathbf{h}} (F_{i+1}^n - F_i^n) + \Delta t H_i^n. \quad (18)$$

We follow this with a backward corrector step which determines the final values at t_{n+1} ,

$$U_i^{n+1} = \frac{1}{2} \left[U_i^n + \bar{U}_i^{n+1} - \frac{\Delta t}{\Delta \mathbf{h}} (\bar{F}_i^{n+1} - \bar{F}_{i+1}^{n+1}) + \Delta t \bar{H}_i^{n+1} \right]. \quad (19)$$

The corrector step corresponds to inserting

$$\mathbf{f}_{i+\frac{1}{2}}^{n+\frac{1}{2}} \equiv \frac{1}{2}(\mathbf{F}_{i+1}^n + \overline{\mathbf{F}}_i^{n+1}), \quad (20)$$

$$\text{and } H_i^{n+\frac{1}{2}} \equiv \frac{1}{2}(H_i^n + \overline{H}_i^{n+1}) \quad (21)$$

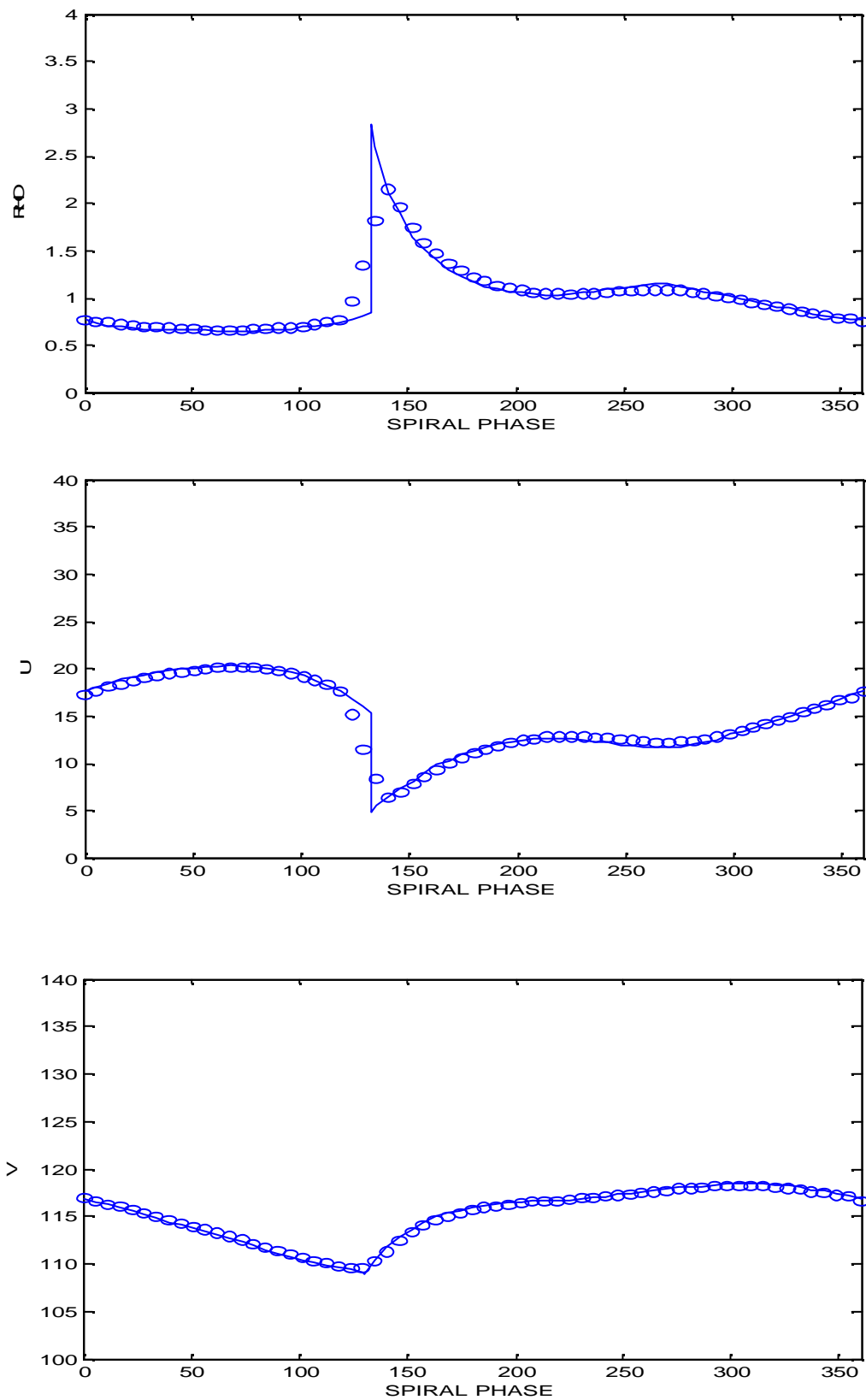
into (13). On the other hand, on odd time-steps we apply a backward predictor step followed by a forward corrector step.

Even though MacCormack's method is slightly dissipative we had to add an explicit smoothing term in order to control nonlinear instabilities in the test problem. The term that we added was

$$D_i^n = b \frac{\Delta t}{\Delta \mathbf{h}} \left[v_{i+\frac{1}{2}}^n (U_{i+1}^n - U_i^n) - v_{i-\frac{1}{2}}^n (U_i^n - U_{i-1}^n) \right]. \quad (22)$$

We applied this to the right hand side of (19). The coefficient b is an adjustable constant of order unity which we take to be 1.10 in this paper. We choose the artificial coefficient to be $v_{i+\frac{1}{2}}^n = |u_{i+1}^n - u_i^n|$ where u is the velocity component mentioned earlier.

In our results we see that our smooth region is modelled well by the MacCormack method however the shock is not very sharp and is quite wide compared to other methods in our study.

Figure one: Result's from MacCormack's method

b) SECOND-ORDER FLUX-SPLITTING METHOD (as in the previous paper [12])

In this method we change a first-order upwind-differencing method into a second-order method by first advancing the cell-boundary values and source terms to the time level $t_{n+\frac{1}{2}}$. In calculating these intermediate values we can ignore the interaction

between the cells (this was observed by Hancock(1980)).

We take Q to be a vector of quantities (not necessarily conserved) describing the state of the gas.

$$Q = \begin{pmatrix} Q \\ u \\ v \end{pmatrix} = \begin{pmatrix} Q \\ q \end{pmatrix} \quad (23)$$

We then assume that the initial values for Q form a piecewise linear distribution so that

$$Q^n(\mathbf{h}) = Q_i^n + (\mathbf{h} - \mathbf{h}_i) \frac{(dQ)_i^n}{\Delta \mathbf{h}} \quad \mathbf{h}_{i-\frac{1}{2}} < \mathbf{h} < \mathbf{h}_{i+\frac{1}{2}} \quad (24)$$

with

$$(dQ)_i^n = c \cdot \text{ave} \left(\frac{q_{i+1}^n - q_i^n}{c}, \frac{q_i^n - q_{i-1}^n}{c} \right) \quad (25)$$

and

$$(dQ)_i^n = Q_i^n \cdot \text{ave} \left(2 \frac{(Q_{i+1}^n - Q_i^n)}{(Q_{i+1}^n + Q_i^n)}, 2 \frac{(Q_i^n - Q_{i-1}^n)}{(Q_i^n + Q_{i-1}^n)} \right) \quad (26)$$

where $\text{ave}(a,b)$ is defined at the end of this methods description.

The formulation of (26) ensures positivity of Q when it is substituted into (24).

Therefore we have

$$\left(\frac{\partial Q}{\partial \mathbf{h}}\right)_i^n = \frac{(\mathbf{d}Q)_i^n}{\Delta \mathbf{h}} \quad (27)$$

allowing us to calculate $\left(\frac{\partial Q}{\partial t}\right)_i^n$ from the appropriate modification of (5) (as shown in

the appendix).

The source terms have already been advanced. Now, we advance the cell averages to

$t_{n+\frac{1}{2}}$ and calculate boundary values using the following equations:

$$Q_i^{n+\frac{1}{2}} = Q_i^n + \frac{\Delta t}{2} \left(\frac{\partial Q}{\partial t}\right)_i^n \quad (28)$$

$$Q_{(i\pm\frac{1}{2})\mu}^{n+\frac{1}{2}} = Q_i^{n+\frac{1}{2}} \pm \frac{\Delta \mathbf{h}}{2} (\mathbf{d}Q)_i^n \quad (29)$$

$$U_{(i\pm\frac{1}{2})\mu}^{n+\frac{1}{2}} = U(Q_{(i\pm\frac{1}{2})\mu}^{n+\frac{1}{2}}) \quad (30)$$

We can now compute the time-centred fluxes at the cell boundary $i \pm \frac{1}{2}$ from $U_{(i\pm\frac{1}{2})\mu}^{n+\frac{1}{2}}$

and $U_{(i\pm\frac{1}{2})\mu}^{n+\frac{1}{2}}$ by any upwind-biased numerical flux formula. We will use a formula, due

to Van Leer (1981b) [14], which is based on flux-vector splitting.

We define the forward and backward fluxes of mass and momentum using

$$F^+(U) = \begin{cases} F(U) & u \geq c \\ \begin{pmatrix} \frac{Q}{4c}(u+c)^2 \\ \frac{Q}{2}(u+c)^2 \\ \frac{Q}{4c}(u+c)^2 v \\ 0 \end{pmatrix} & |u| < c \\ 0 & u \leq -c \end{cases} \quad (31)$$

and $F(U) = F^-(U) + F^+(U)$.

The numerical flux for this method being

$$\mathbf{f}_{i+\frac{1}{2}}^{n+\frac{1}{2}} = F^+(U_{(i+\frac{1}{2})-}^{n+\frac{1}{2}}) + F^-(U_{(i+\frac{1}{2})+}^{n+\frac{1}{2}}). \quad (32)$$

The local stability condition is a combination of

$$\frac{\Delta t}{\Delta \mathbf{h}} (|u| + \mathbf{m}c)_i \leq 1 \quad \text{with } \mathbf{m} = 1, \quad (33)$$

$$\text{and } \frac{\Delta t}{\Delta \mathbf{h}} c_i \leq \frac{1}{2}.$$

The function $ave(a,b)$ is chosen such that it tends to $\frac{1}{2}(a+b)$ if a and b are

subsequent finite differences of a smooth solution, but when the solution is not

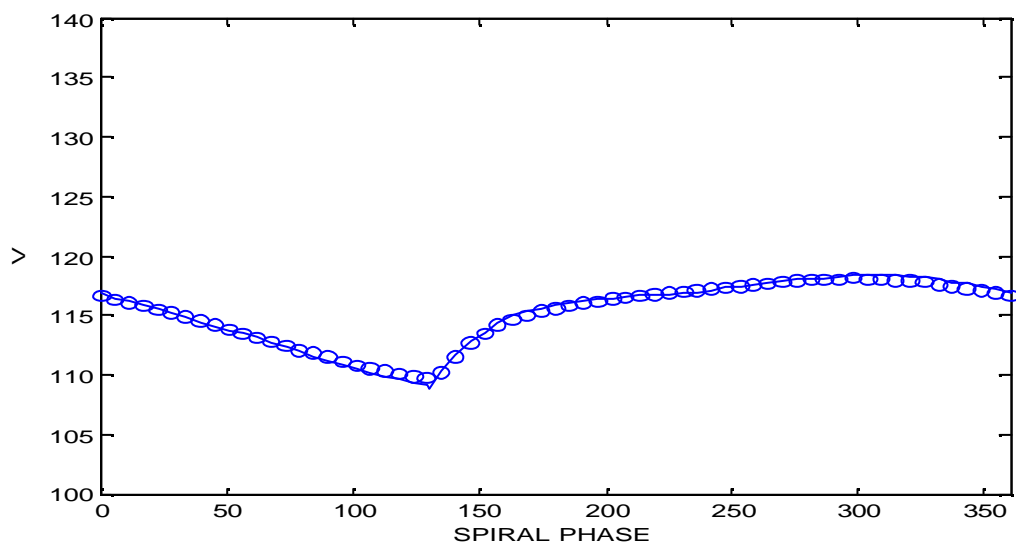
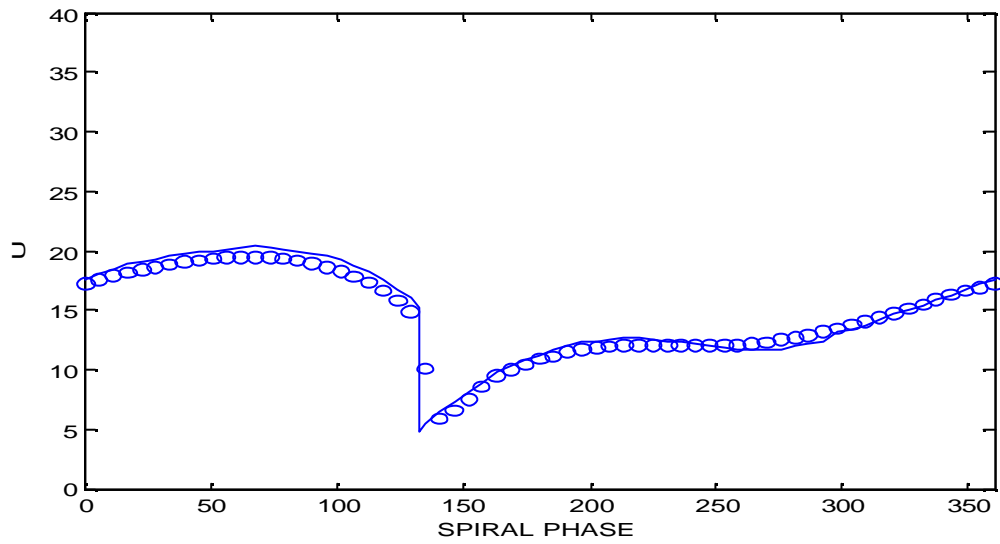
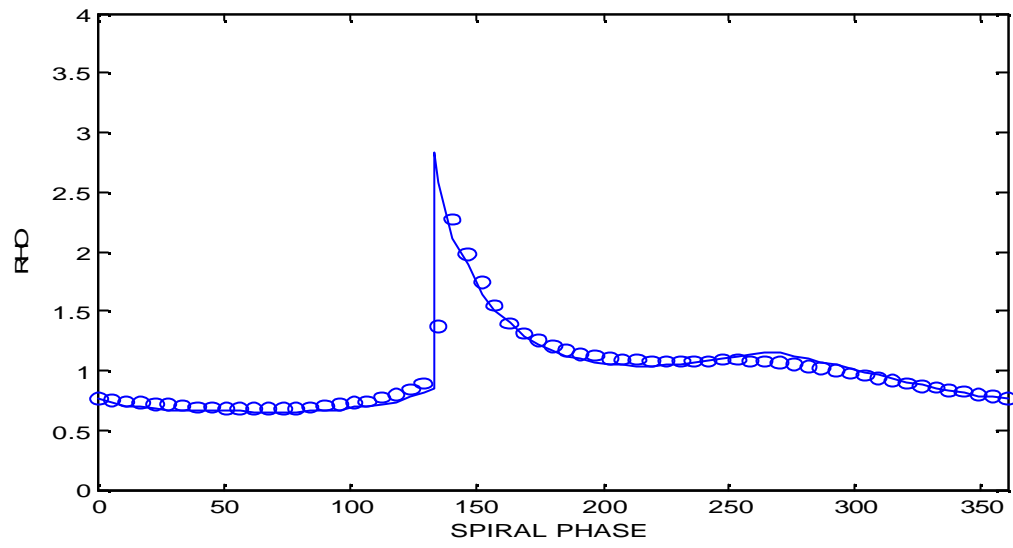
smooth it tends to the smallest value (see Van Leer,1977 [13]),

$$ave(a,b) = \frac{(b^2 + \mathbf{e}^2)a + (a^2 + \mathbf{e}^2)b}{a^2 + b^2 + 2\mathbf{e}^2} \quad (34)$$

where \mathbf{e}^2 is a small non-vanishing bias of the order $O((\Delta \mathbf{h})^3)$.

In the actual computations we used $\mathbf{e}^2 = 0.008$, but the results are not very sensitive to its precise value.

In our results we see that the smooth region is modelled reasonably accurately and our shock is sharper and narrower than the shock produced by MacCormack's method.

Figure two: Results from the second-order flux-splitting method

GODUNOV'S METHOD

Godunov's method considers the numerical values of the solution to be the cell averages of the analytic solution and so to have a piecewise constant distribution. It then goes on to solve the exact Riemann problems at each of the cell boundaries over the following time step. It averages the end solutions to return to a uniform constant distribution and this cycle is repeated.

APPROXIMATE RIEMANN SOLVERS (see Leveque [3])

All the methods in this paper excluding (a) and (b) are approximate Riemann solvers. Approximate Riemann solvers were developed because Godunov's method and the higher order variations of this method require us to solve Riemann problems at every cell boundary on each time step. This is very expensive and typically requires some iteration for nonlinear equations. After computing the Riemann problem we go on to average over each time step and so lose most of the structure of the resulting Riemann solver. This introduces large numerical errors. We therefore consider approximate Riemann solvers to be a possible alternative as they may produce equally good results with less expense.

For given data Q_i and Q_{i-1} , an approximate Riemann solution might define a function

$\hat{Q}_{i-\frac{1}{2}}\left(\frac{x}{t}\right)$ that approximates the true similarity solution to the Riemann problem with

data Q_i and Q_{i-1} . This function will typically consist of some set of M_w waves $W_{i-\frac{1}{2}}^p$

propagating at some speeds $s_{i-\frac{1}{2}}^p$, with

$$Q_i - Q_{i-1} = \sum_{p=1}^{M_w} W_{i-\frac{1}{2}}^p. \quad (35)$$

We can generalise Godunov's method using this function by taking one of the following approaches.

1. We begin by setting

$$F_{i-\frac{1}{2}} = f\left(\hat{Q}_{i-\frac{1}{2}}^\downarrow\right) \quad (36)$$

where $\hat{Q}_{i-\frac{1}{2}}^\downarrow = \hat{Q}_{i-\frac{1}{2}}(0) = Q_{i-1} + \sum_{\substack{p: s_{i-\frac{1}{2}}^p < 0 \\ i-\frac{1}{2}}} W_{i-\frac{1}{2}}^p$ is the value along the cell interface.

We then take

$$A^- \Delta Q_{i-\frac{1}{2}} = f\left(\hat{Q}_{i-\frac{1}{2}}^\downarrow\right) - f(Q_{i-1}), \quad (37)$$

$$A^+ \Delta Q_{i-\frac{1}{2}} = f(Q_i) - f\left(\hat{Q}_{i-\frac{1}{2}}^\downarrow\right), \quad (38)$$

and substitute these values into the following equation

$$Q_i^{n+1} = Q_i^n - \frac{\Delta t}{\Delta h} \left(A^+ \Delta Q_{i-\frac{1}{2}} + A^- \Delta Q_{i+\frac{1}{2}} \right). \quad (39)$$

2. We use the waves and speeds from the approximate Riemann solution to define:

$$A^- \Delta Q_{i-\frac{1}{2}} = \sum_{p=1}^{M_w} \left(s_{i-\frac{1}{2}}^p \right)^- W_{i-\frac{1}{2}}^p, \quad (40)$$

$$A^+ \Delta Q_{i-\frac{1}{2}} = \sum_{p=1}^{M_w} \left(s_{i-\frac{1}{2}}^p \right)^+ W_{i-\frac{1}{2}}^p, \quad (41)$$

and use them in (39).

b) ROE'S SCHEME

Roe proposed a method which approximates the system

$$u_t + f_x = 0,$$

by using a piecewise constant approximation in each cell

$$u(x, t) = \begin{cases} u_L & \text{if } \mathbf{h}_L - \frac{\Delta \mathbf{h}}{2} < \mathbf{h} < \mathbf{h}_L + \frac{\Delta \mathbf{h}}{2}, \\ u_R & \text{if } \mathbf{h}_R - \frac{\Delta \mathbf{h}}{2} < \mathbf{h} < \mathbf{h}_R + \frac{\Delta \mathbf{h}}{2}. \end{cases} \quad (42)$$

where u_L and u_R are piecewise constant states at t_n and then determines the solution of the following linearised problem:

$$u_t + \tilde{A}(u_L, u_R)u_x = 0. \quad (43)$$

In this linearised problem we have $\tilde{A}(u_L, u_R) = \frac{\partial f}{\partial u}$

where $\tilde{A}(u_l, u_r)$ needs to satisfy the following conditions:

- i) $\tilde{A}(u_l, u_r)(u_r - u_l) = f(u_r) - f(u_l)$ (conservation)
- ii) $\tilde{A}(u_l, u_r)$ is diagonalisable with real eigenvalues (hyperbolicity)
- iii) $\tilde{A}(u_l, u_r) \rightarrow f'(\bar{u})$ smoothly as $u_l, u_r \rightarrow \bar{u}$ (consistency)

As shown in the appendix we find that for this problem the Roes averages are as follows

$$\tilde{A}(u_l, u_r) = \begin{pmatrix} 0 & 1 & 0 \\ c^2 - \bar{u}^2 & 2\bar{u} & 0 \\ -\bar{u}\bar{v} & \bar{v} & \bar{u} \end{pmatrix} \quad (44)$$

where

$$\bar{u} = \frac{\sqrt{Q_r}u_r + \sqrt{Q_l}u_l}{\sqrt{Q_r} + \sqrt{Q_l}} \quad \text{and} \quad \bar{v} = \frac{\sqrt{Q_r}v_r + \sqrt{Q_l}v_l}{\sqrt{Q_r} + \sqrt{Q_l}}. \quad (45)$$

We now find the eigenvalues and eigenvectors of our matrix (as shown in the appendix). Once we have completed these calculations we observe that in this problem we have a contact discontinuity (an eigenvalue being u).

We take our numerical flux function in this method to be

$$H(u_l, u_r) = \frac{1}{2}(f(u_l) + f(u_r)) - \sum_{p=1}^m |\hat{\mathbf{I}}_p| \mathbf{a}_p \hat{r}_p \quad (46)$$

where

\mathbf{I}_p are the eigenvalues,

r_p are the right eigenvectors,

and

$$\mathbf{a}_p = l_p(u_r - u_l)$$

where l_p are the left eigenvectors.

Therefore our numerical flux function works out to be

$$H(u_l, u_r) = \frac{1}{2}(f(u_l) + f(u_r)) - \frac{1}{2} \left[\left(\frac{(c - \bar{u})\mathbf{d}_1 + (\bar{u} + c)\mathbf{d}_2 - 2c\bar{v}\mathbf{d}_3}{2c} \right) |\bar{u} + c| \begin{pmatrix} 1 \\ \bar{u} + c \\ \bar{v} \end{pmatrix} + \left(\frac{\mathbf{d}_1 - \mathbf{d}_2}{2c} \right) |\bar{u} - c| \begin{pmatrix} 1 \\ \bar{u} - c \\ \bar{v} \end{pmatrix} + \mathbf{d}_3 |\bar{u}| \begin{pmatrix} 0 \\ 0 \\ 1 \end{pmatrix} \right].$$

We work the source terms out separately.

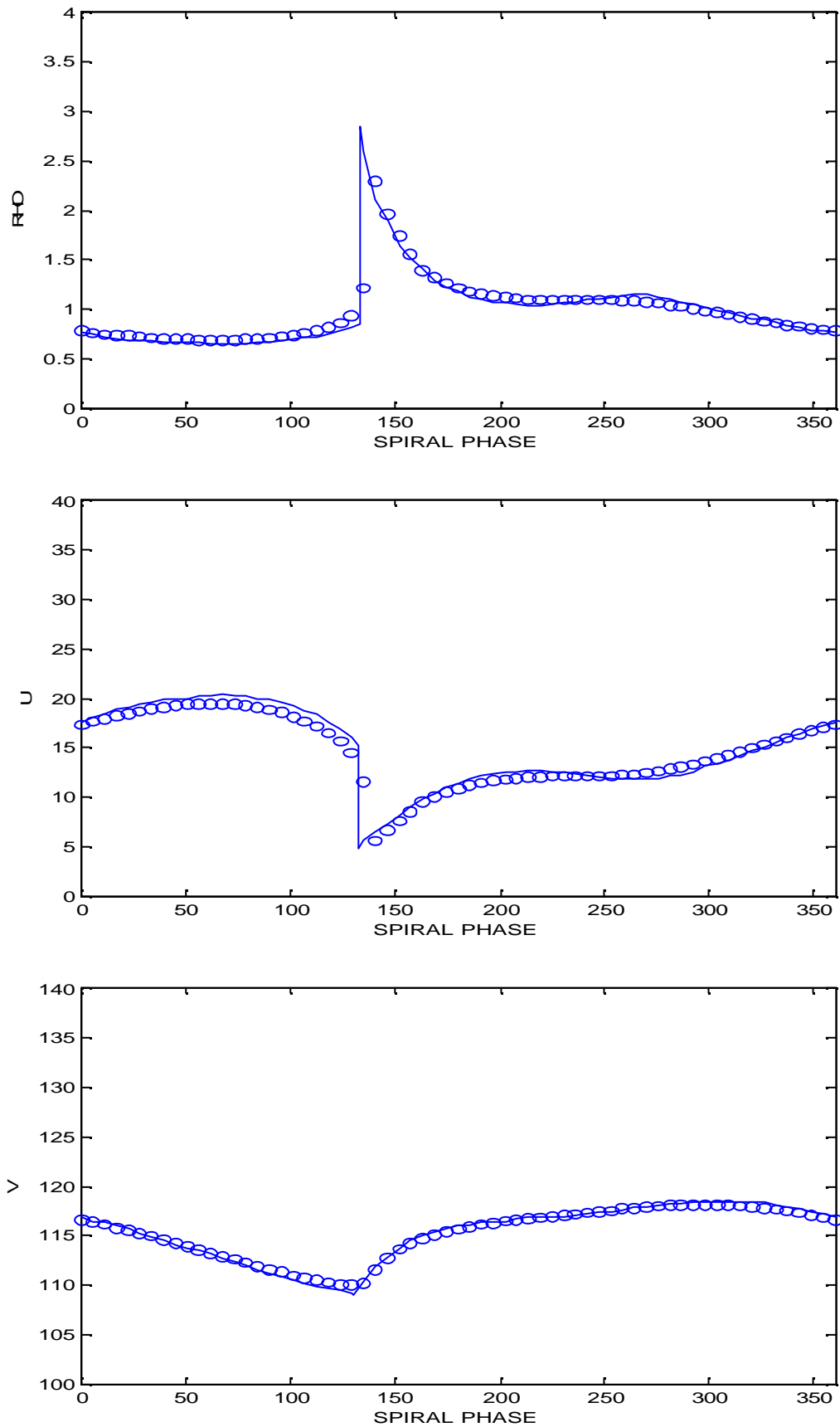
This method only uses shocks in the solution and is not entropy satisfying. However entropy fixes do exist.

STABILITY

For this scheme to remain stable we require that:

$$\frac{\Delta t}{\Delta \mathbf{h}} \max(|\mathbf{I}_k|) \leq 1. \quad (47)$$

In the results we see that this method models the general features of the smooth zone and produces a shock which is similar to that produced by the second-order flux-splitting method.

Figure three: Results from Roe's Scheme

d) ROE'S SCHEME WITH FLUX LIMITERS

In these methods we apply a limited anti-diffusive flux to Roe's scheme.

Flux limiters are functions of the ratio of consecutive gradients of the solution.

We begin by choosing a high order flux f_H that works well in smooth regions and a low order flux f_L that behaves well near discontinuities. We then try to hybridise these two fluxes into a single flux f .

This is implemented as follows

1. We view the high order flux as

$$f_H = f_L + (f_H - f_L) \quad (48)$$

(i.e. it is equivalent to the low order flux plus a correction term)

2. We apply our flux limiter to the correction term as below

$$f = f_L + \mathbf{f}(\mathbf{q})(f_H - f_L) \quad (49)$$

We use the limiter to try to alter the flux in relation to the data so that our method produces good results.

The correction term is often known as the antidiffusive flux (as above) since the low order flux contains too much diffusion for the smooth data and the correction term compensates.

All the flux limiter functions that we shall study are high-resolution second-order TVD limiters and are defined as below:

$$\text{Minmod: } \mathbf{f}(\mathbf{q}) = \max(0, \min(\mathbf{q}, 1)); \quad (50)$$

Superbee: $\mathbf{f}(\mathbf{q}) = \max(0, \min(1, 2\mathbf{q}), \min(2, \mathbf{q}))$; (51)

MC: $\mathbf{f}(\mathbf{q}) = \max(0, \min((1 + \mathbf{q})/2, 2, 2\mathbf{q}))$; (52)

Van Leer: $\mathbf{f}(\mathbf{q}) = \frac{\mathbf{q} + |\mathbf{q}|}{1 + |\mathbf{q}|}$. (53)

Our limited antidiffusive flux in this case is as follows:

$$\tilde{F}_{i-\frac{1}{2}} = \frac{1}{2} \sum_{p=1}^m |\mathbf{l}^p| \left(1 - \frac{\Delta t}{\Delta h} |\mathbf{l}^p|\right) \tilde{\mathbf{a}}_{i-\frac{1}{2}}^p r^p \quad (54)$$

in which

\mathbf{l}^p are the eigenvalues (as before),

r^p are the right eigenvectors (as before),

and

$$\tilde{\mathbf{a}}_{i-\frac{1}{2}}^p = l^p (u_i - u_{i-1}) \mathbf{f}(\mathbf{q}_{i-\frac{1}{2}}^p) \quad (55)$$

where

l^p are the left eigenvectors,

and

$$\mathbf{q}_{i-\frac{1}{2}}^p = \frac{\mathbf{a}_{i-\frac{1}{2}}^p}{\mathbf{a}_{i-\frac{1}{2}}^p} \quad \text{with} \quad \mathbf{I} = \begin{cases} i-1 & \text{if } \mathbf{l}^p > 0, \\ i+1 & \text{if } \mathbf{l}^p < 0. \end{cases} \quad (56)$$

First, we looked at using the minmod limiter over all the characteristic fields and then went onto vary the limiters we used particularly concentrating on our contact field.

RESULTS FOR TEST ONE

Roe's scheme with minmod limiter:

This has a sharp, reasonably narrow shock and a smooth zone that is modelled well.

Roe's scheme with Van Leer limiter applied to the contact field and minmod applied elsewhere:

This has a sharp, reasonably narrow shock and a smooth zone that is modelled well.

Roe's scheme with superbee limiter applied to the contact field and minmod applied elsewhere:

This has a sharp and narrow shock and a smooth zone that is modelled very well.

Also, when we apply this method to uniform initial values and look at the results after 30,000 time steps we see that our values have started blowing up.

Roe's scheme with MC limiter:

The results of this method are very similar to those we obtained from Roe's scheme with the superbee limiter applied to the contact field and minmod applied elsewhere.

We therefore have omitted these graphs.

Roe's scheme with Van Leer limiter:

The results of this method are very similar to those we obtained from Roe's scheme with the Van Leer limiter applied to the contact field and minmod applied elsewhere.

We therefore have omitted these graphs.

In the results we see that these methods are a substantial improvement on the Roe scheme without limiters applied. The smooth zone is modelled very well and the shocks produced are sharp and narrow. The best results are produced by the method

with the MC limiter applied and the method with the minmod and superbee limiters applied. These two methods were chosen for test two. Also shown are the results these schemes produced after thirty thousand time steps when we start from uniform initial values. From these graphs we see that our results blow up after a certain amount of time and therefore may not be the best methods to use for this problem.

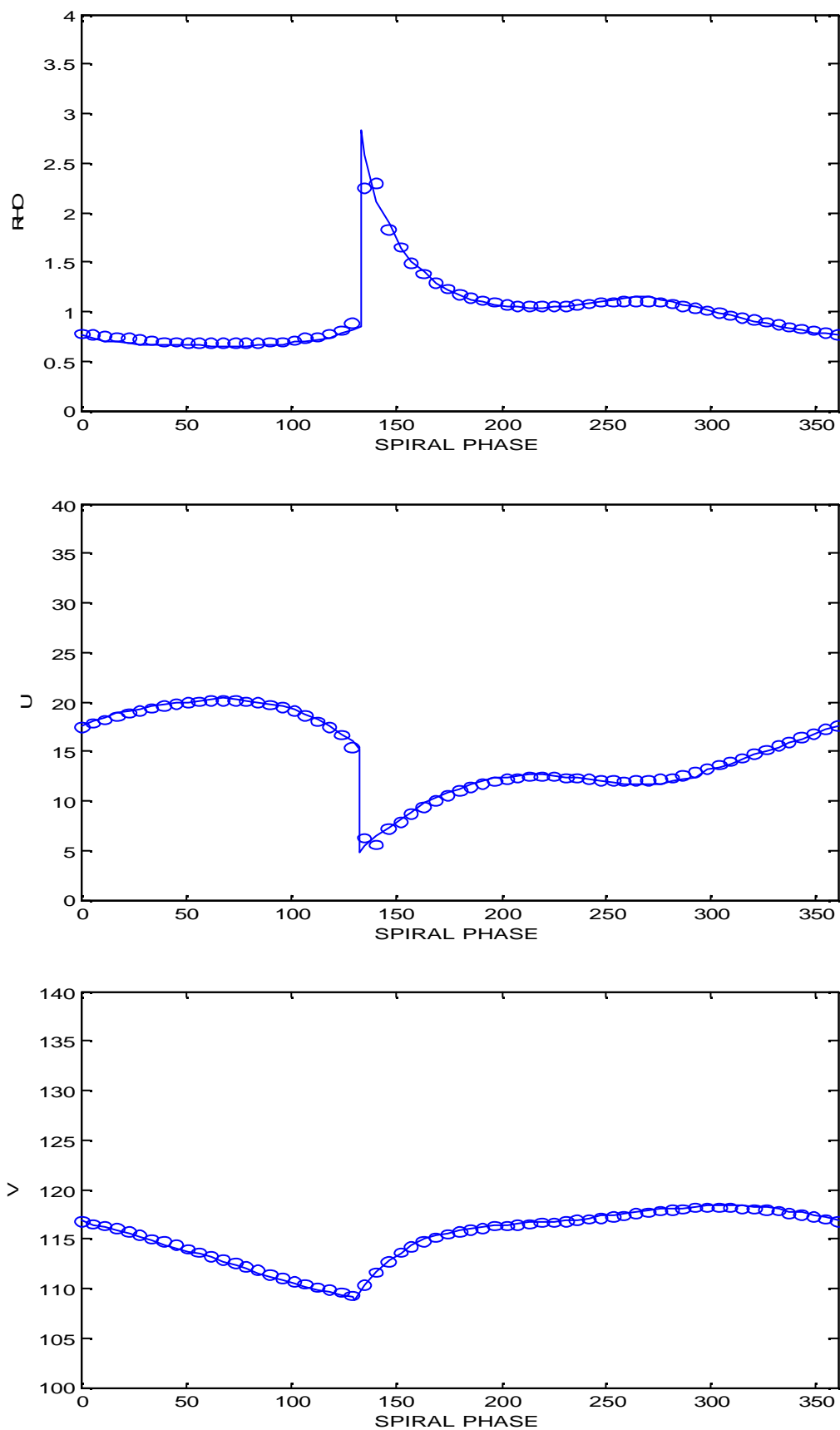
Figure four: Results from Roe's scheme with minmod limiter

Figure five: Results from Roe's scheme with Van Leer limiter applied to the contact field and minmod applied elsewhere.

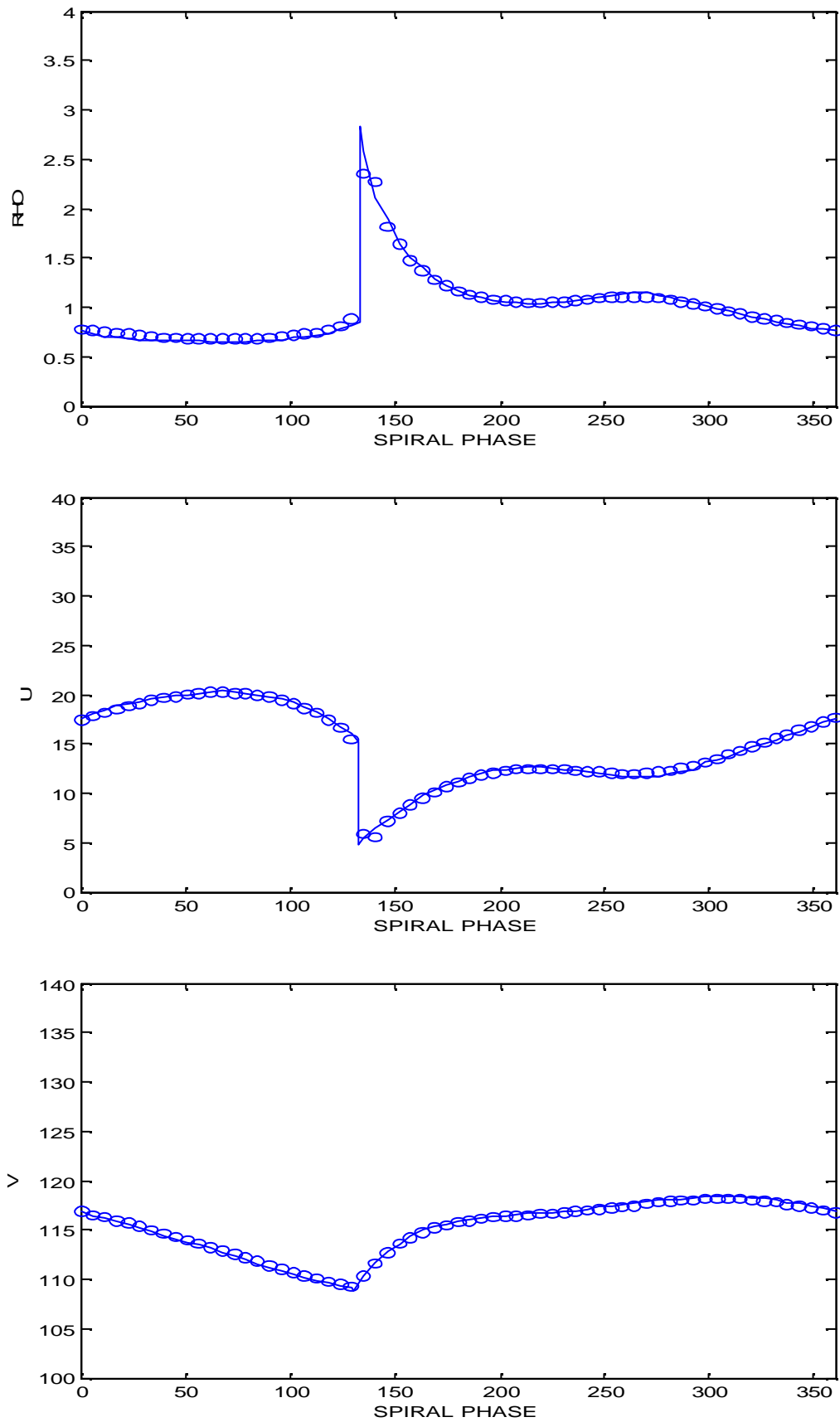
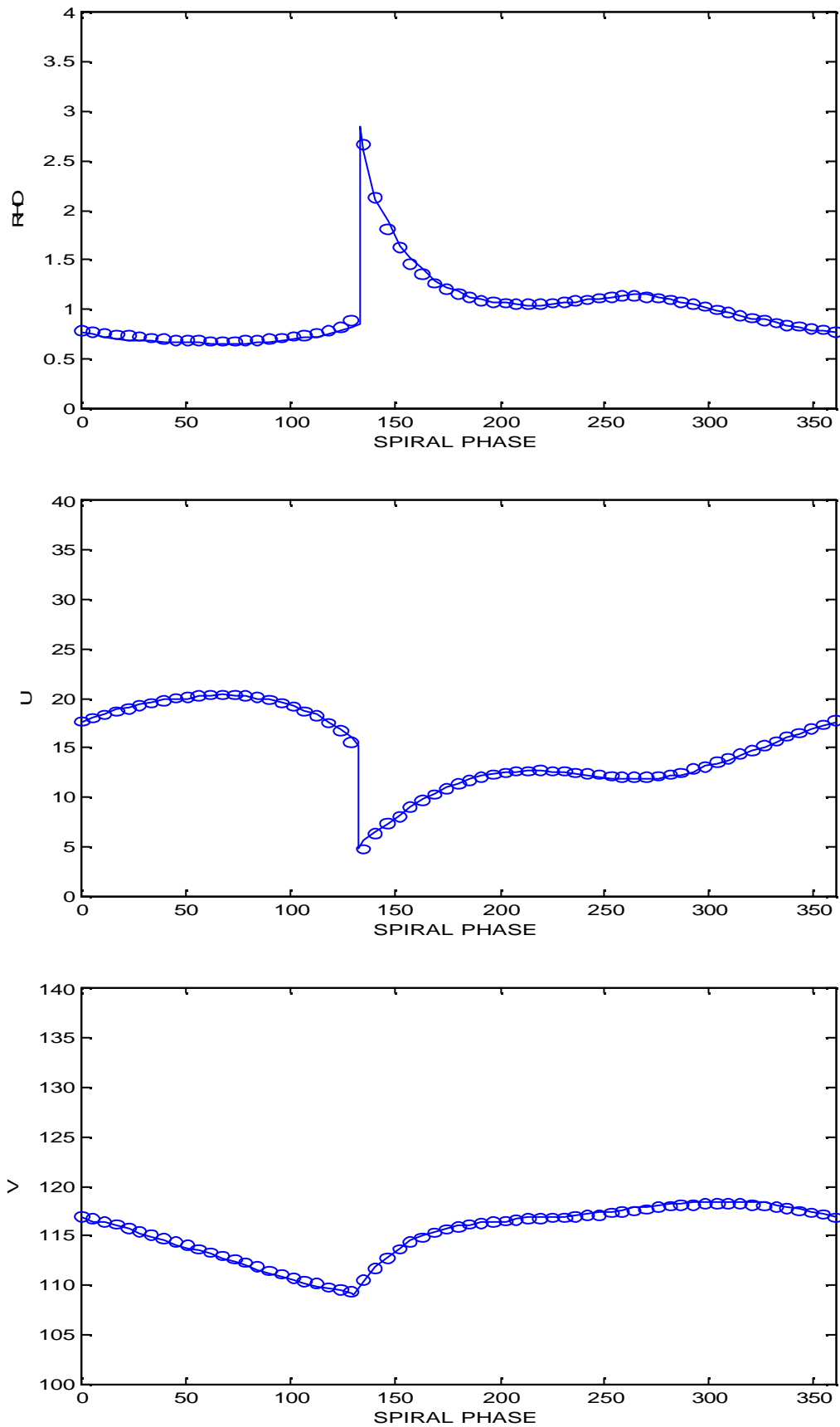
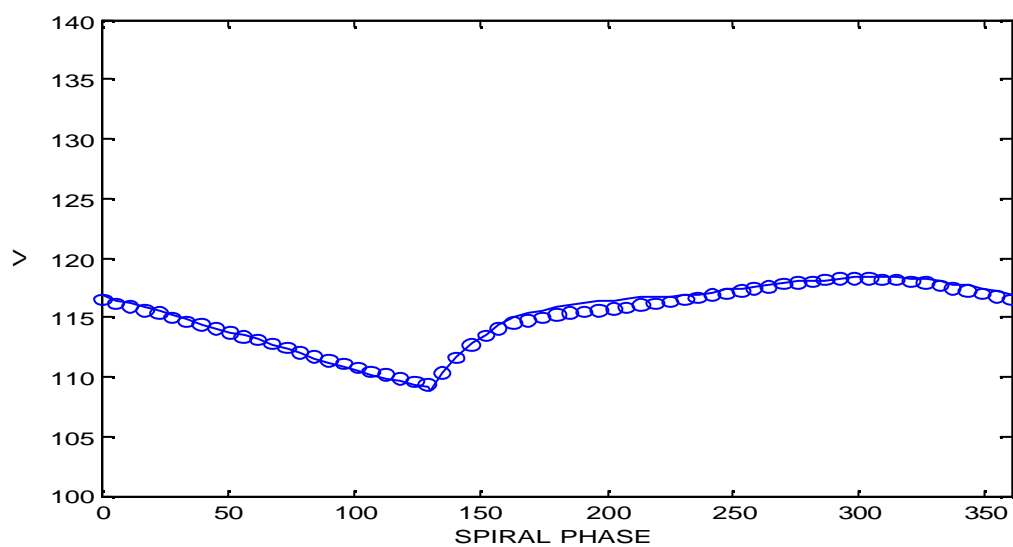
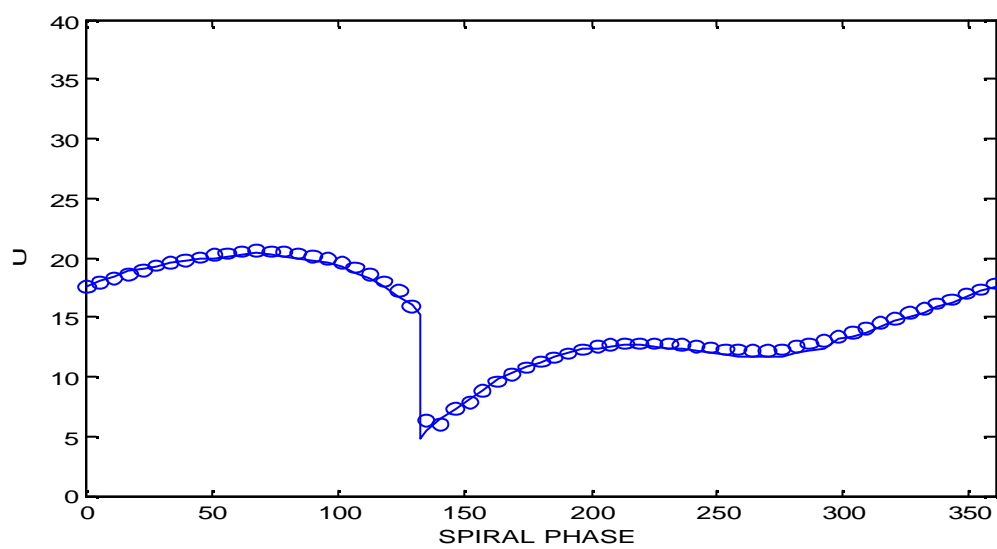
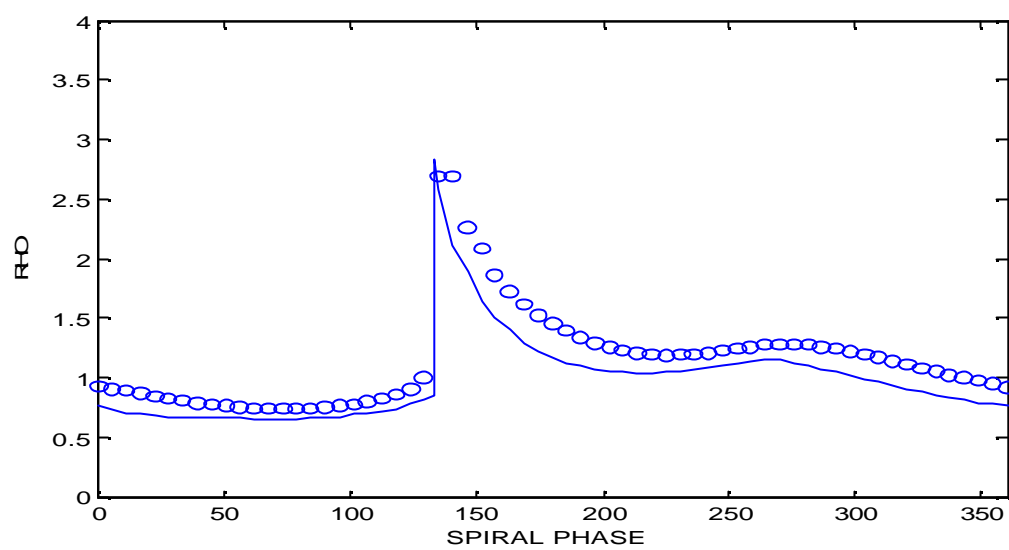


Figure six: Results from Roe's scheme with superbee applied to the contact field and minmod applied elsewhere.



After 30,000 time steps using uniform initial values



e) ROE'S SCHEME WITH THE SOURCE TERM DECOMPOSED AND FLUX

LIMITERS APPLIED

We go on to consider this method since it is thought to create a balance between the flux and source term in the steady state and so satisfy the C-property of Bermudez and Vazquez.

We can decompose the source terms as we have decomposed the flux terms. If we do this we have that

$$\tilde{R} = \frac{1}{\Delta x} \sum_{k=1}^p \tilde{\mathbf{b}}_k \tilde{\epsilon}_k \quad (57)$$

where $\tilde{\mathbf{b}}_k$ are the coefficients of the decomposition of the source terms onto the eigenvectors of the characteristic decomposition.

From this we can approximate the source term by the following

$$R_i^* = R_{i+\frac{1}{2}}^- + R_{i-\frac{1}{2}}^+ \quad (58)$$

where

$$R_{i+\frac{1}{2}}^\pm = \frac{1}{2} \sum_{k=1}^p \left[\tilde{\mathbf{b}}_k \tilde{\epsilon}_k (1 \pm \text{sgn}(\tilde{\mathbf{I}}_k) (1 - \Phi_k (1 - |\mathbf{n}_k|))) \right]_{i+\frac{1}{2}} \quad (59)$$

and $\Phi_k = \mathbf{f}(\mathbf{q}_{i-\frac{1}{2}}^k)$.

RESULTS FOR TEST ONE

Roe's scheme with the source term decomposed:

This has a sharp, reasonably narrow shock and a smooth zone that is modelled well.

Roe's scheme with the source term decomposed and MC limiter applied:

This has a narrow, reasonably sharp shock and a smooth zone that is modelled well.

Roe's scheme with the source term decomposed and Van Leer limiter applied:

This has a narrow, reasonably sharp shock and a smooth zone that is modelled well.

Roe's scheme with the source term decomposed and minmod limiter applied:

This has a sharp and narrow shock and a smooth zone that is modelled well.

Also, when we apply this method to uniform initial values the results are still close to the exact solution after 30,000 time steps.

Roe's scheme with the source term decomposed, the Van Leer limiter applied to the contact field and minmod applied elsewhere:

The results of this method are very similar to those we obtained from Roe's scheme with the source term decomposed and the Van Leer limiter applied.

We therefore have omitted these graphs.

Roe's scheme with the source term decomposed, the superbee limiter applied to the contact field and minmod applied elsewhere:

The results of this method are very similar to those we obtained from Roe's scheme with the source term decomposed and the MC-limiter applied.

We therefore have omitted these graphs.

We see similarly good results from these methods as we did in (d) however there are some differences. We have a sharper shock with the minmod limited scheme and blunter shocks with the method using the MC-limiter as well as the method using a combination of the minmod and superbee limiters. Our best results obtained in this section is from the scheme using the minmod limiter. Test two was therefore performed on this scheme.

As before we also look at how the results have progressed after 30,000 time steps (using uniform initial values) for the minmod limited scheme. We see that these results do not blow up as they did in the previously studied methods and therefore conclude that this may be a better method for this problem.

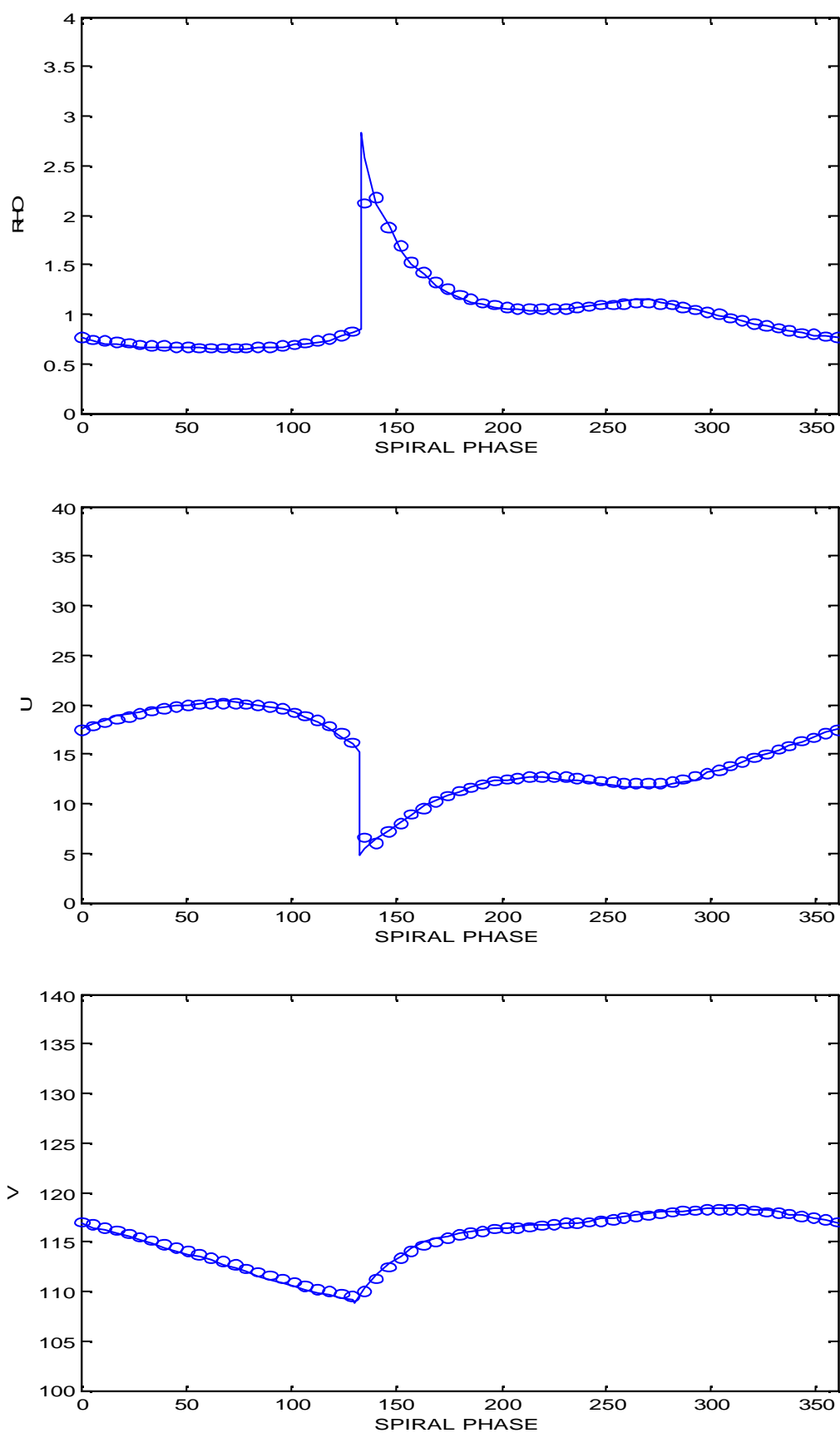
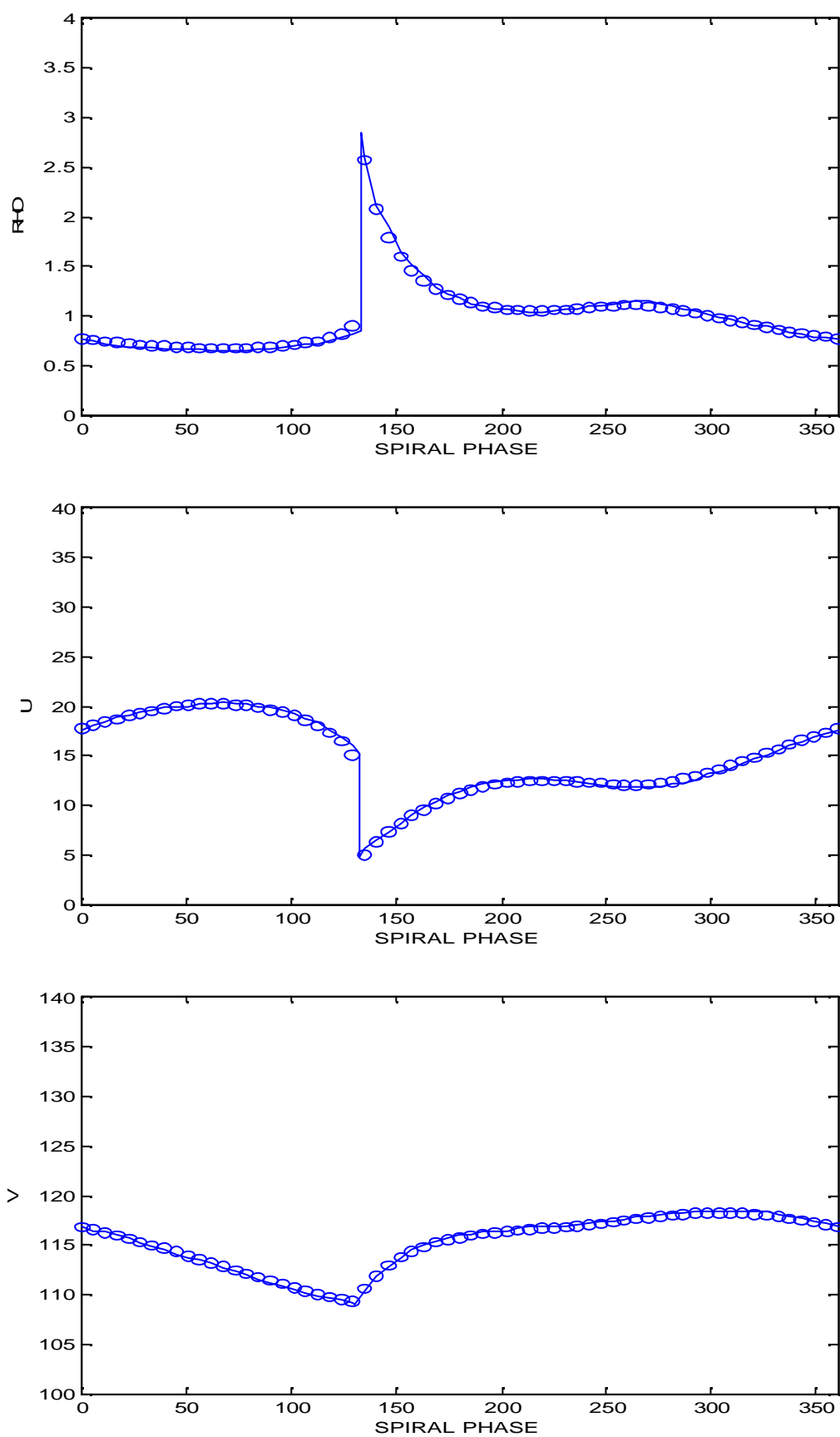
Figure seven: Results from Roe's scheme with the source term decomposed

Figure eight: Results from Roe's scheme with the source term decomposed and minmod limiter applied.



After 30,000 time steps using uniform initial values

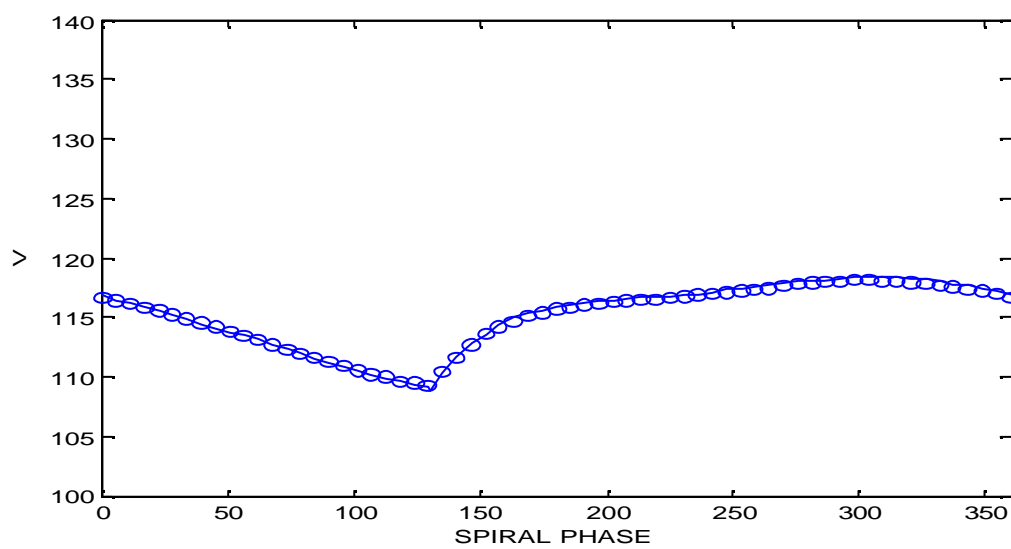
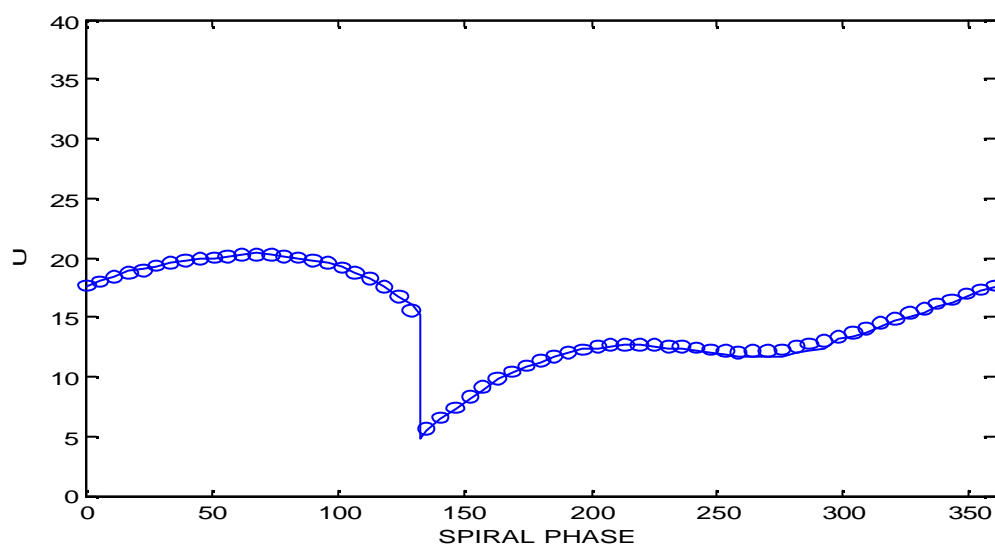
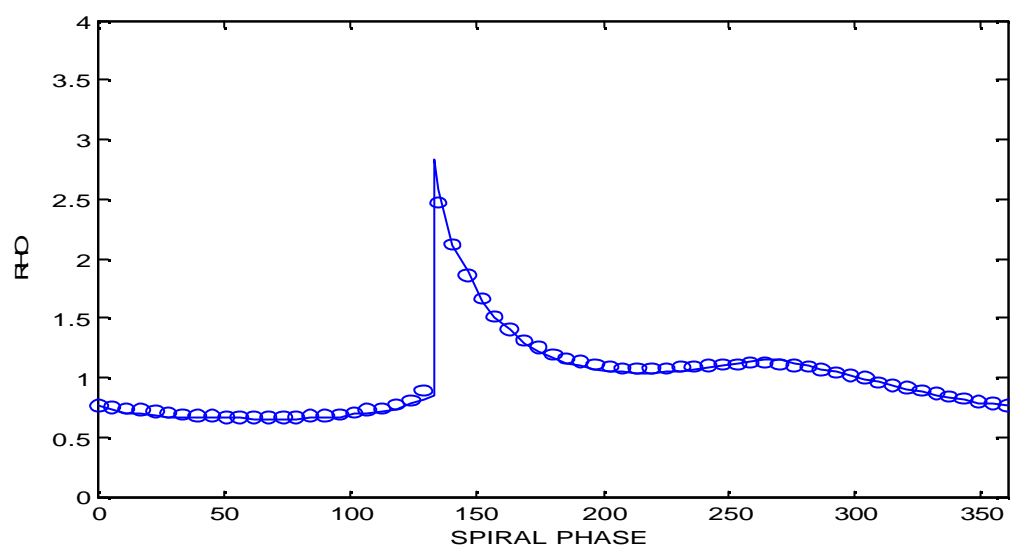


Figure nine: Results from Roe's scheme with the source term decomposed and MC limiter applied.

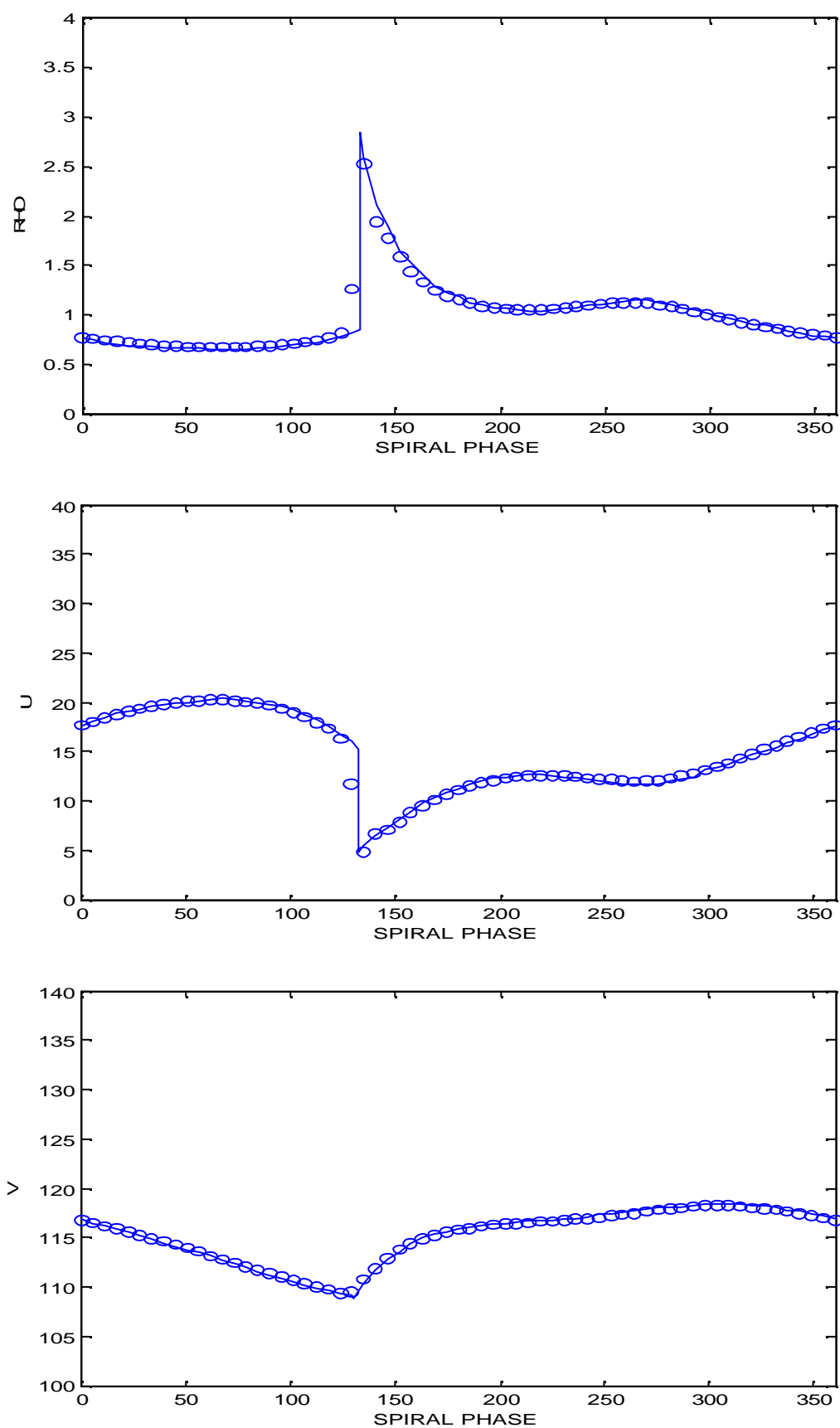
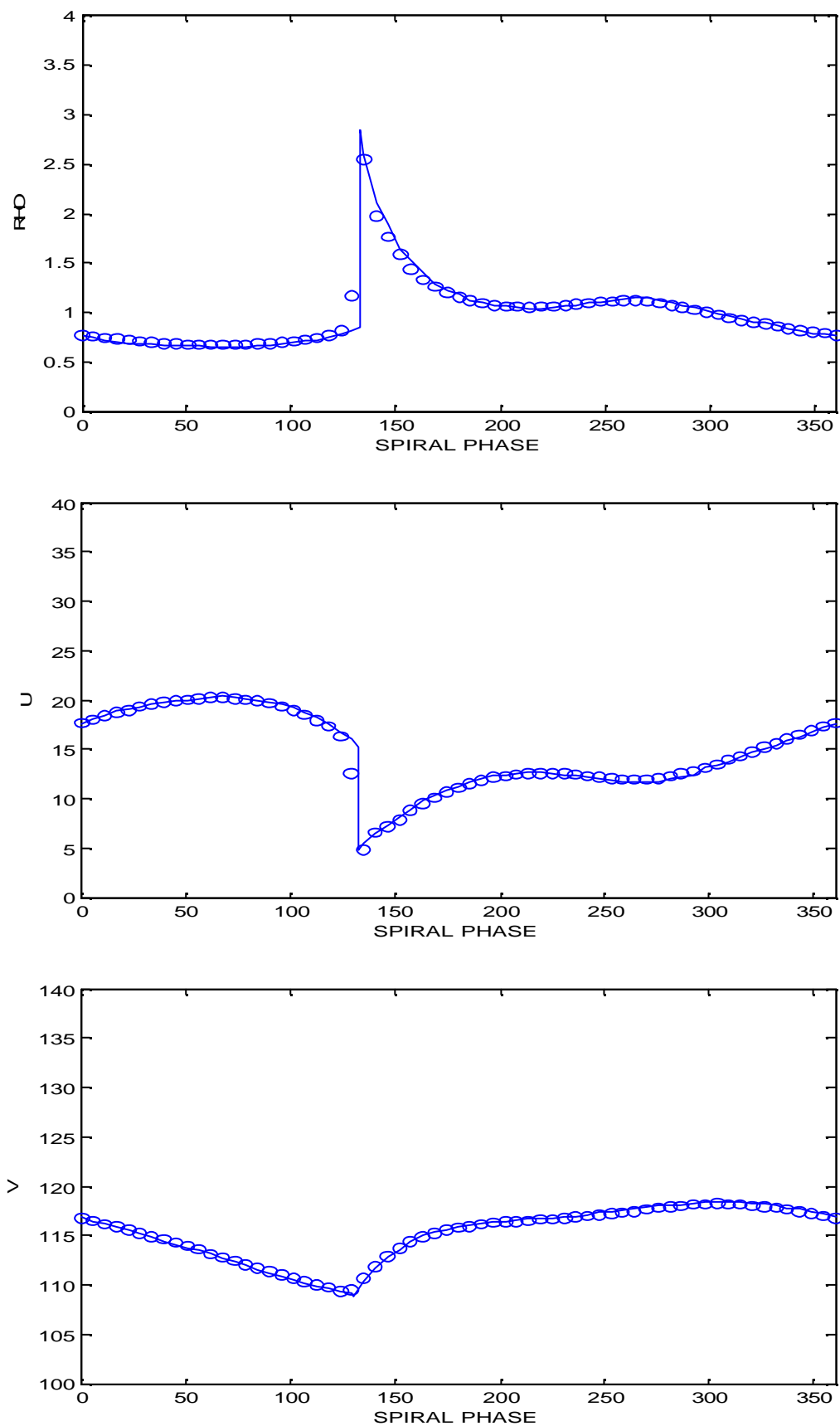


Figure ten: Results from Roe's scheme with the source term decomposed and Van Leer limiter applied.



f) HLL SCHEME

Harten, Lax and Van Leer proposed this approach for solving the Riemann problem approximately.

In this method we obtain an approximation for the intercell flux directly. We assume a wave configuration for the solution that consists of two waves separating three constant states. Taking the wave speeds to be given by one of the following algorithms, application of the integral form of the conservation laws gives a closed-form, approximate expression for the flux.

Possible algorithms for the wave speeds (signal velocities) are:

$$\begin{aligned}
 1. \quad S_L &= u_L - c, & S_R &= u_R + c; \\
 2. \quad S_L &= \min(u_L - c, u_R - c), & S_R &= \max(u_L + c, u_R + c); \\
 3. \quad S_L &= \bar{u} - c, & S_R &= \bar{u} + c.
 \end{aligned} \tag{60}$$

where \bar{u} is our Roe average.

The HLL flux is

$$F^{hll} = \frac{S_R F_L - S_L F_R + S_L S_R (U_R - U_L)}{S_R - S_L}. \tag{61}$$

The corresponding intercell flux for the approximate Godunov method is

$$F_{i+\frac{1}{2}}^{hll} = \begin{cases} F_L & \text{if } 0 \leq S_L, \\ \frac{S_R F_L - S_L F_R + S_L S_R (U_R - U_L)}{S_R - S_L} & \text{if } S_L \leq 0 \leq S_R, \\ F_R & \text{if } 0 \geq S_R. \end{cases} \tag{62}$$

STABILITY

The numerical flux function may also be written in the following form

$$F_{i+\frac{1}{2}}^{hl} = \frac{1}{2} \left[f(u_i) + f(u_{i+1}) - Q_{i+\frac{1}{2}} (u_{i+1} - u_i) \right] \quad (63)$$

where $Q_{i+\frac{1}{2}}$ (the numerical viscosity-matrix) is defined by

$$Q_{i+\frac{1}{2}} = \frac{S_R + S_L}{S_R - S_L} A(u_L, u_R) - 2 \frac{S_R S_L}{S_R - S_L} I \quad (64)$$

when $A(u_L, u_R)$ is a Roe-type linearization which has real eigenvectors $\mathbf{a}_{i+\frac{1}{2}}^k$, a complete set of eigenvectors and satisfies the property

$$F_R - F_L = A(u_L, u_R)(u_R - u_L).$$

Now, a necessary condition for stability is that the viscosity matrix (as defined above) has nonnegative eigenvalues where the eigenvalues are defined as below:

$$\mathbf{s}_{i+\frac{1}{2}}^k = \frac{S_+ (\mathbf{a}_{i+\frac{1}{2}}^k - S_-) - S_- (S_+ - \mathbf{a}_{i+\frac{1}{2}}^k)}{S_+ - S_-} \quad (k=1,2,3) \quad (65)$$

where $S_+ = \max(0, S_R)$ and $S_- = \min(0, S_L)$.

Therefore, a necessary stability condition for the signal velocities is as follows:

$$\mathbf{s}_{i+\frac{1}{2}}^k \geq 0, \quad (66)$$

this is satisfied if

$$S_- \leq \mathbf{a}_{i+\frac{1}{2}}^k \leq S_+$$

RESULTS FOR TEST ONE

HLL using the first algorithm for the wave speeds:

This has a reasonably sharp shock which is displaced downstream and captures the most general features of the smooth zone.

HLL using the second algorithm for the wave speeds :

This has a shock which isn't modelled very well and captures the most general features of the smooth zone.

HLL using the third algorithm for the wave speeds :

This has a sharp, reasonably narrow shock and captures the most general features of the smooth zone.

In the results we see that the third algorithm for the wave speeds is the best method to choose for this problem. The shock in this method is slightly sharper than the other two and it models the smooth zone reasonably well. The methods are not as good as the schemes in (d) and (e) at modelling the smooth zone. In the method using the first algorithm we see a shock which is nearly as sharp as the shock produced using the third whereas the second algorithm obtains a much blunter shock than the others.

g) HLL SCHEME WITH THE MINMOD LIMITER APPLIED

When we apply flux limiters to this scheme we use a different method to the one we have previously described in this paper. We apply the limiters to the waves $W_{i-\frac{1}{2}}^p$.

This is implemented as follows

$$\tilde{W}_{i-\frac{1}{2}}^p = \mathbf{f}(\mathbf{q}_{i-\frac{1}{2}}^p) W_{i-\frac{1}{2}}^p, \quad (67)$$

where

$$\mathbf{q}_{i-\frac{1}{2}}^p = \frac{W_{i-\frac{1}{2}}^p \cdot W_{i-\frac{1}{2}}^p}{W_{i-\frac{1}{2}}^p \cdot W_{i-\frac{1}{2}}^p}, \quad W_{i-\frac{1}{2}}^p = \mathbf{a}_{i-\frac{1}{2}}^p r_{i-\frac{1}{2}}^p, \quad I = \begin{cases} i-1 & \text{if } s_{i-\frac{1}{2}}^p > 0, \\ i+1 & \text{if } s_{i-\frac{1}{2}}^p < 0. \end{cases} \quad (68)$$

and $s_{i-\frac{1}{2}}^p$ are wave speeds determined by the HLL method.

Our limited antidiffusive flux here is as below

$$\tilde{F}_{i-\frac{1}{2}} = \frac{1}{2} \sum_{p=1}^m \left| s_{i-\frac{1}{2}}^p \left(1 - \frac{\Delta t}{\Delta x} \left| s_{i-\frac{1}{2}}^p \right| \right) \right| \tilde{W}_{i-\frac{1}{2}}^p. \quad (69)$$

RESULTS FOR TEST ONE

HLL with the minmod limiter applied and using the first algorithm for the wave speeds:

This has a sharp and narrow shock which is displaced downstream. It shows an improvement on the accuracy in the smooth zone that we found without the limiter but is still not one our best methods at modelling this region.

HLL with the minmod limiter and using the second algorithm for the wave speeds:

This has a reasonable sharp and narrow shock. It shows an improvement on the accuracy of the smooth zone that we found without the limiter but is still not one our best methods at modelling this region.

HLL with the minmod limiter and using the third algorithm for the wave speeds:

This has a relatively blunt shock. It shows an improvement on the accuracy of the smooth zone that we found without the limiter but is still not one our best methods at modelling this region.

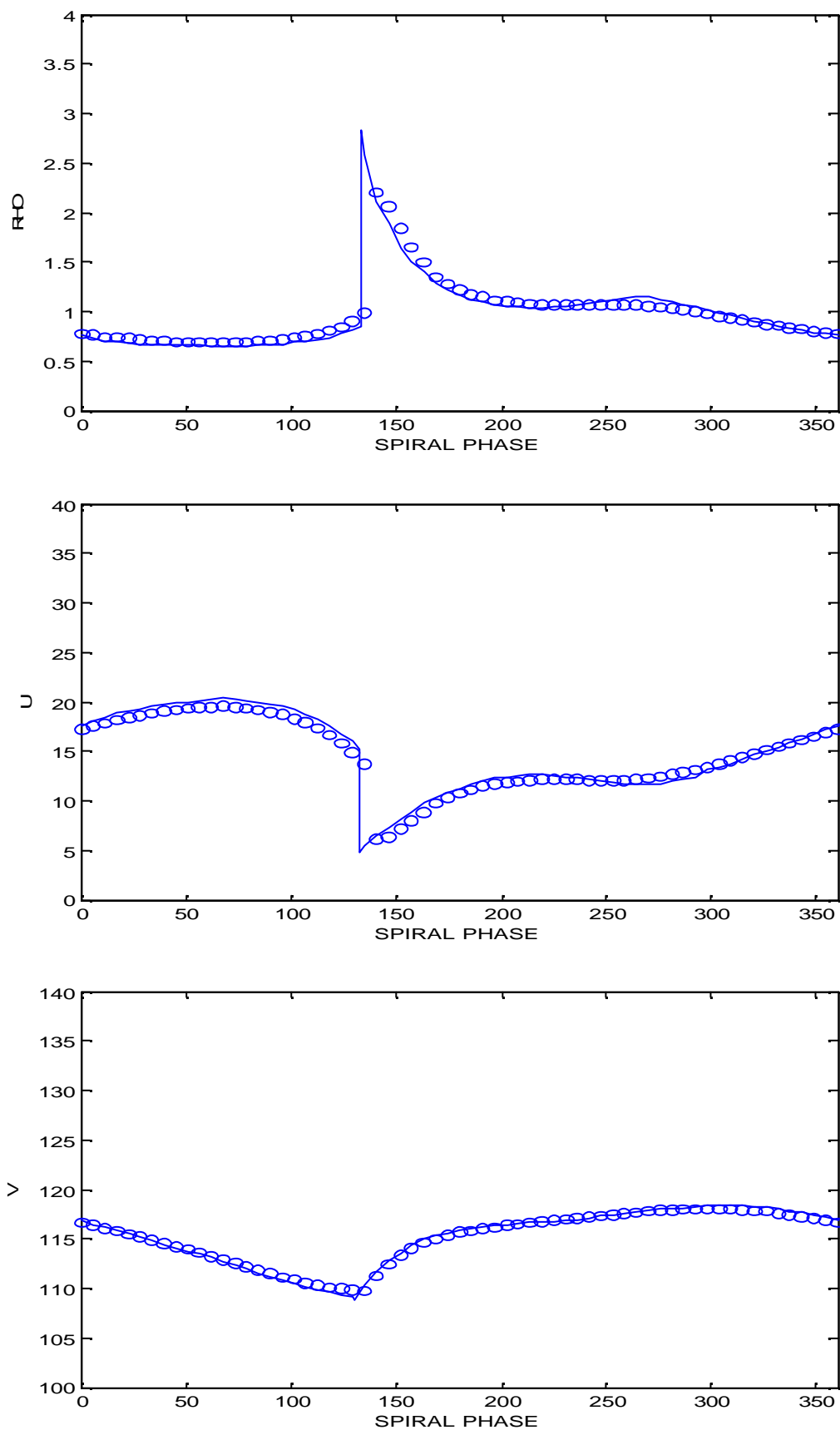
Figure eleven: Results from the HLL Scheme with wave speed algorithm (1)

Figure twelve: Results from the HLL Scheme with the minmod limiter applied and using wave speed algorithm (1)

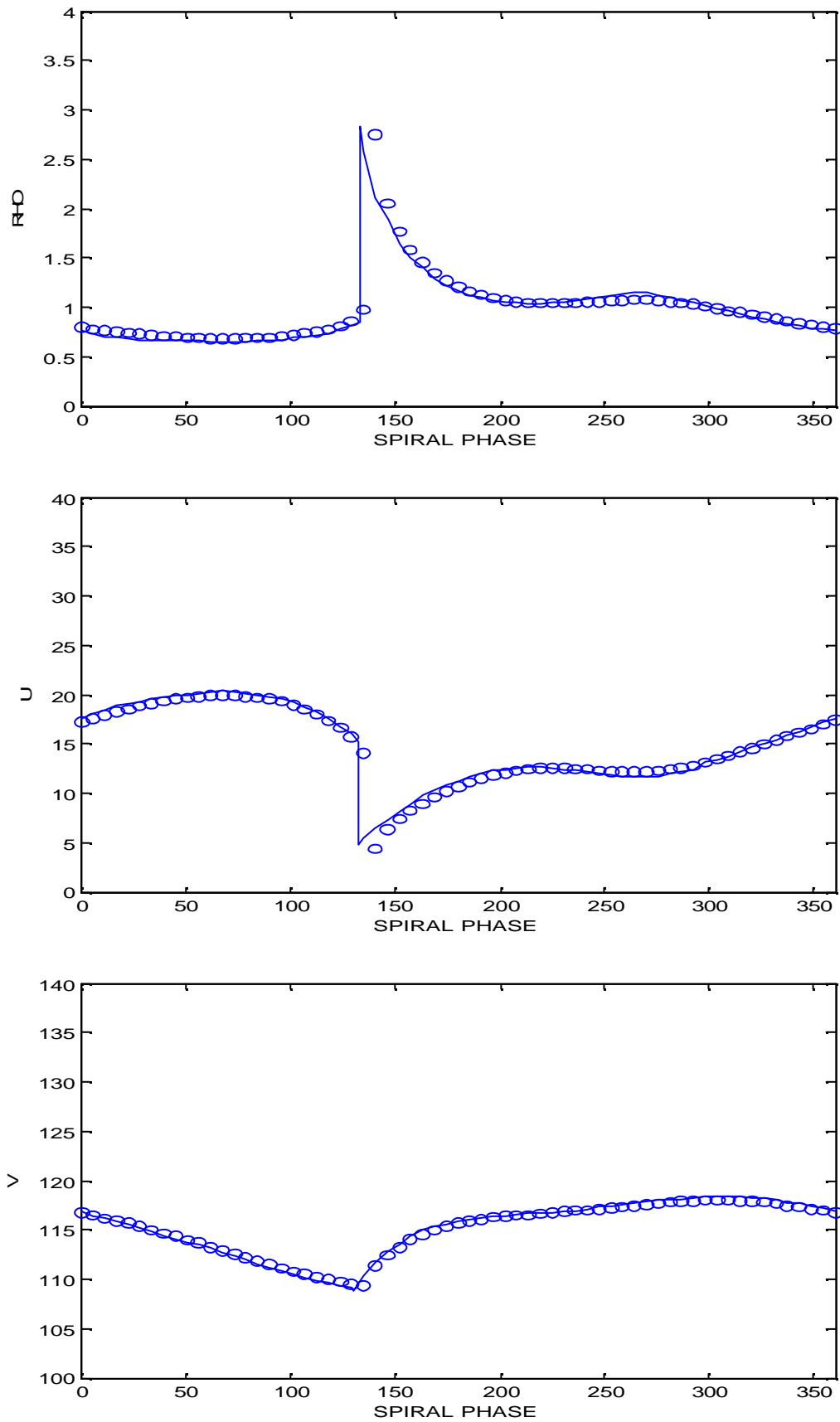


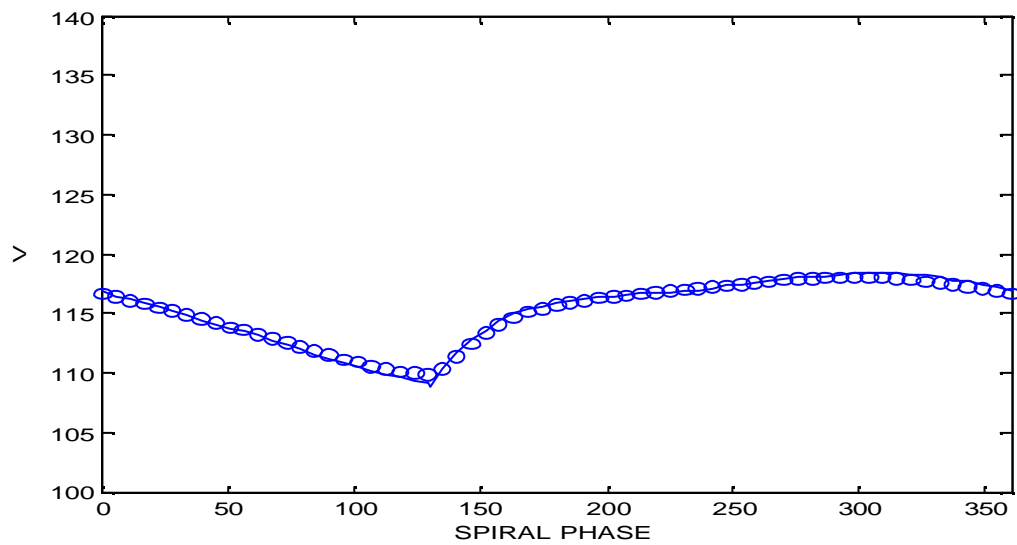
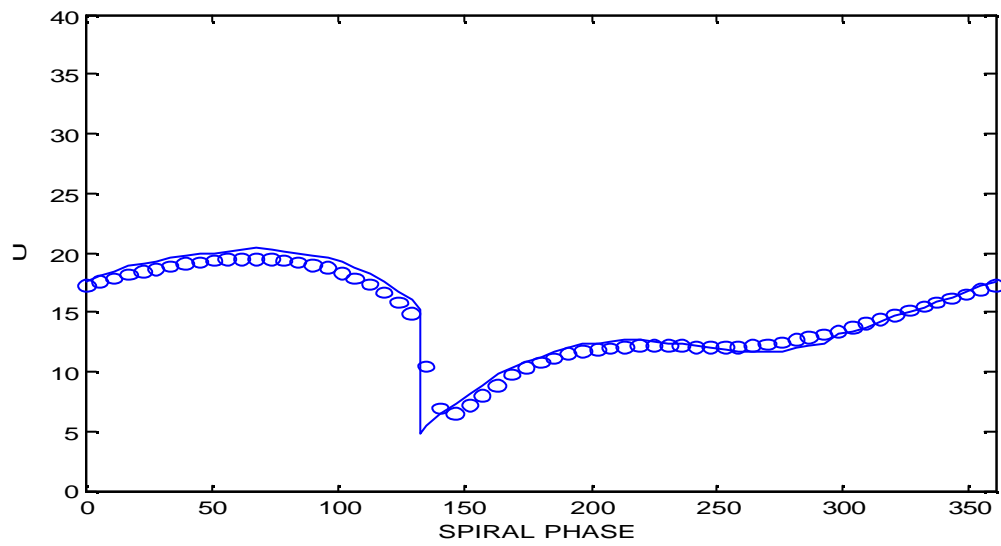
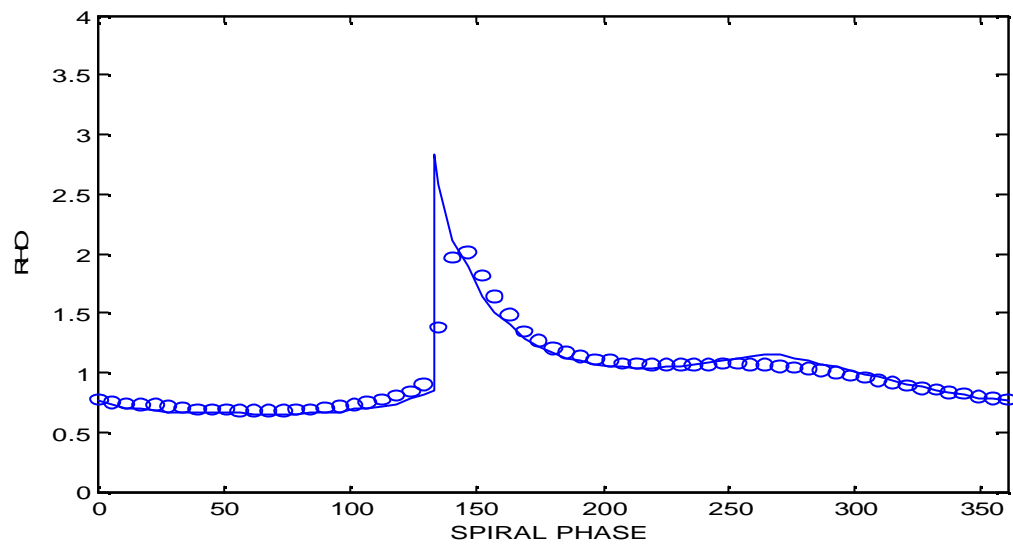
Figure thirteen: Results from the HLL Scheme with wave speed algorithm (2)

Figure fourteen: Results from the HLL Scheme with the minmod limiter applied and using wave speed algorithm (2)

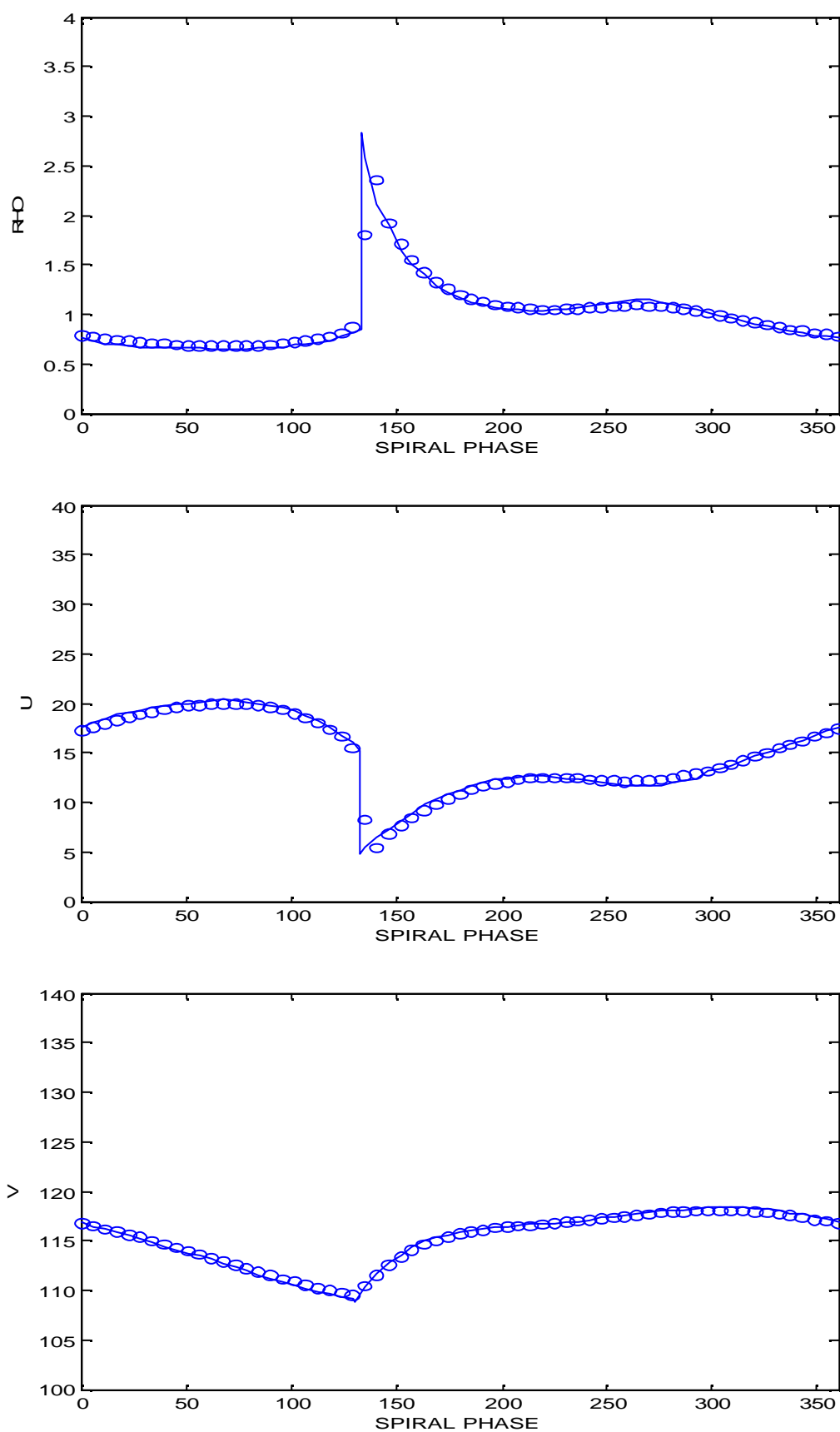


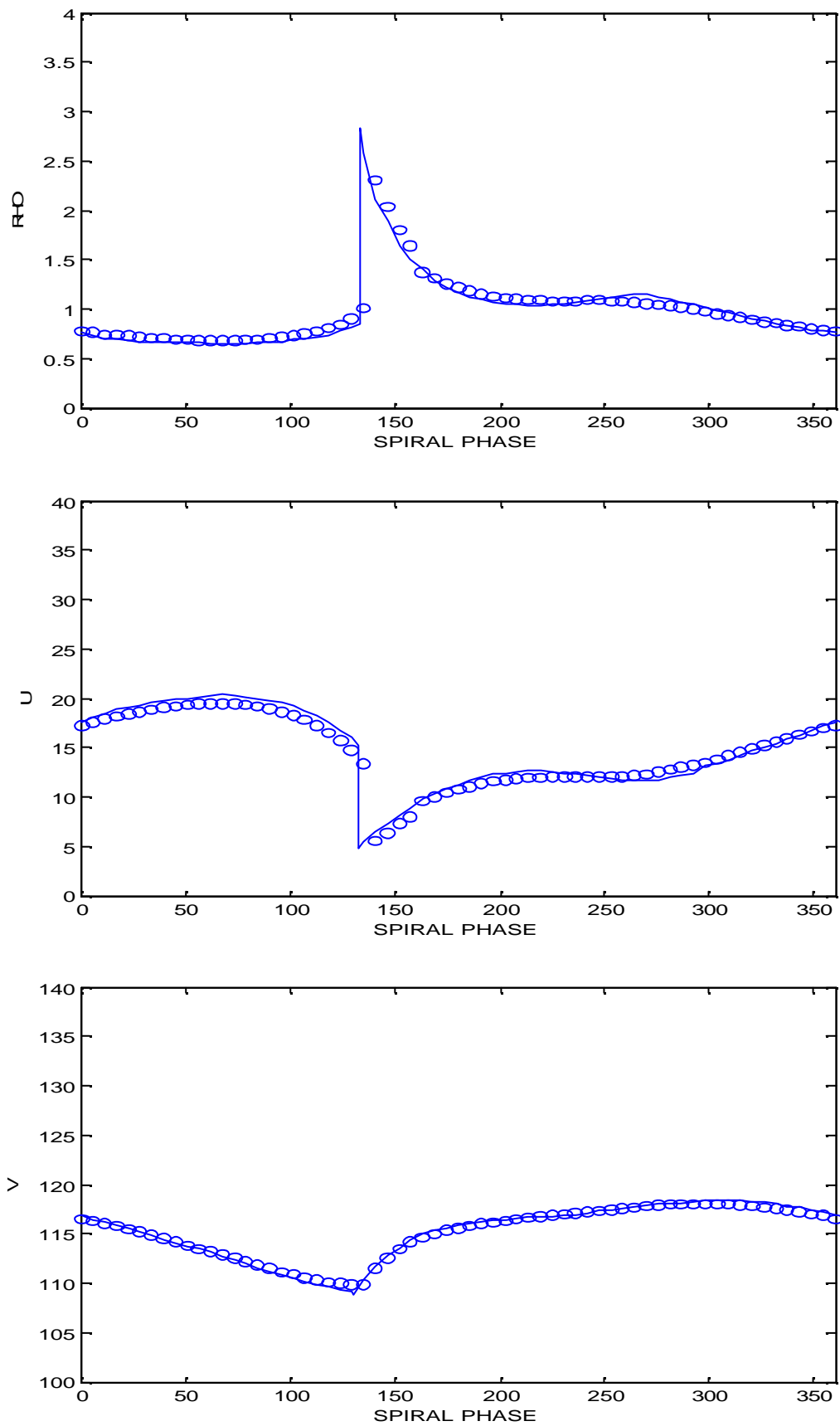
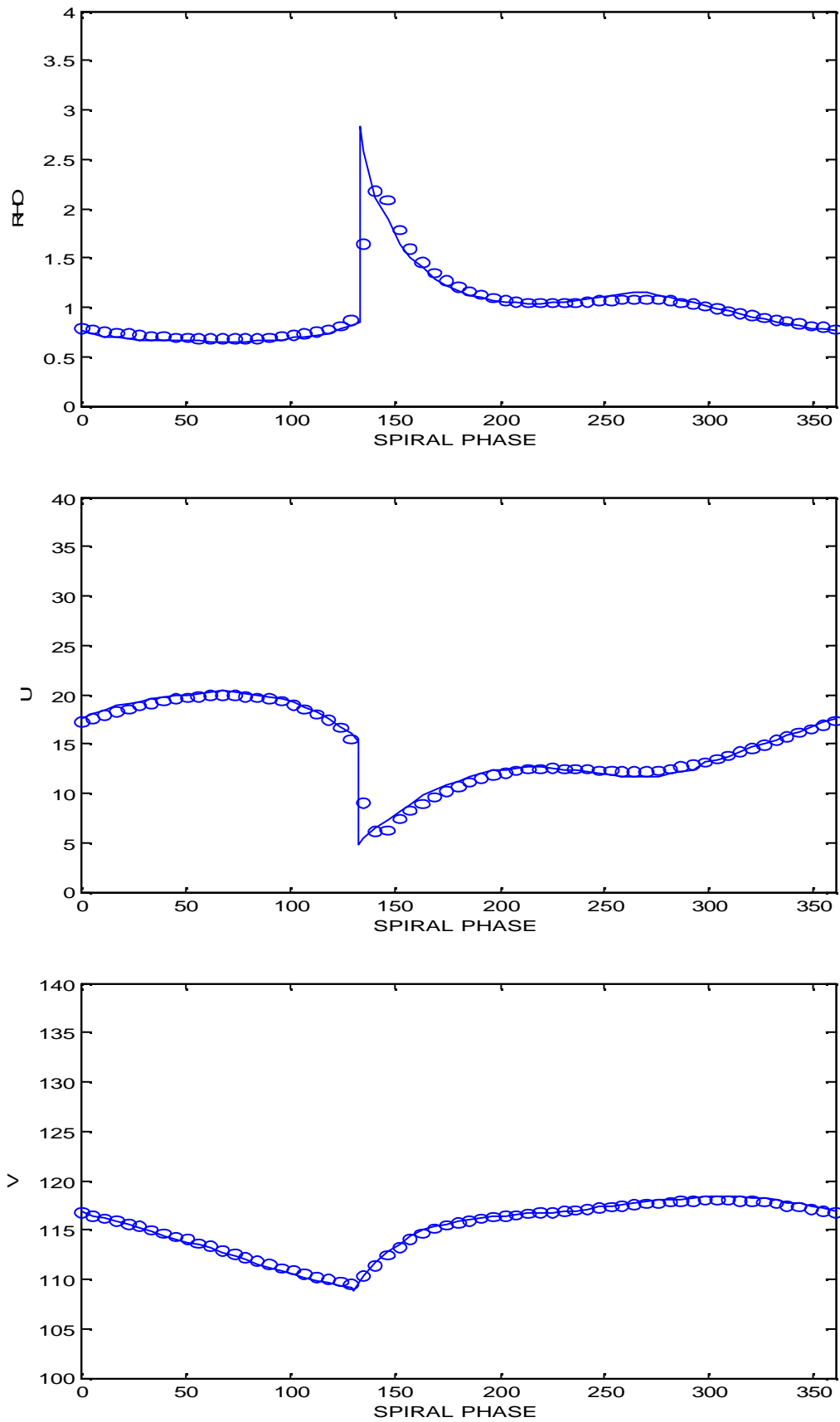
Figure fifteen: Results from the HLL Scheme with wave speed algorithm (3)

Figure sixteen: Results from the HLL Scheme with the minmod limiter applied and using wave speed algorithm (3)



h) HLLC SCHEME

A modification of the HLL scheme is the HLLC method. This was suggested by Toro, Spruce and Spears. It is a better scheme to apply on our problem as we are dealing with a three equation system and so the two-wave assumption is incorrect. The C in HLLC stands for contact. In this method we modify the Riemann solver to obtain a more accurate approximation of our contact discontinuity. We do this by including the middle wave of speed S_* in our calculations in addition to the fastest and slowest (which were used in HLL).

The HLLC approximate solver is as follows:

$$\tilde{U}(x, t) = \begin{cases} U_L & \text{if } \frac{x}{t} \leq S_L, \\ U_{*L} & \text{if } S_L \leq \frac{x}{t} \leq S_*, \\ U_{*R} & \text{if } S_* \leq \frac{x}{t} \leq S_R, \\ U_R & \text{if } \frac{x}{t} \geq S_R. \end{cases} \quad (70)$$

The following conditions are imposed on the approximate Riemann solver:

$$u_{*L} = u_{*R} = u_* \quad \text{and} \quad v_{*L} = v_L, \quad v_{*R} = v_R,$$

$$S_* = u_*.$$

Now, taking

$$U_{*k} = \mathbf{r}_k \begin{pmatrix} S_k - u_k \\ S_k - S_* \end{pmatrix} \begin{pmatrix} 1 \\ S_* \\ v_k \end{pmatrix} \quad \text{for } k = L \text{ and } k = R. \quad (71)$$

the HLLC flux for the approximate Godunov method is

$$F_{i+\frac{1}{2}}^{hllc} = \begin{cases} F_L & \text{if } 0 \leq S_L, \\ F_{*L} = F_L + S_L(U_{*L} - U_L) & \text{if } S_L \leq 0 \leq S_*, \\ F_{*R} = F_R + S_R(U_{*R} - U_R) & \text{if } S_* \leq 0 \leq S_R, \\ F_R & \text{if } 0 \geq S_R. \end{cases} \quad (72)$$

RESULTS FOR TEST ONE

HLLC using the first algorithm for the wave speeds:

This has a sharp, narrow shock which is displaced downstream and captures the most general features of the smooth zone.

HLLC using the second algorithm for the wave speeds:

This has a narrow, reasonably sharp shock and captures the most general features of the smooth zone.

HLLC using the third algorithm for the wave speeds:

This has a relatively blunt shock and captures the most general features of the smooth zone.

In the results we see that the best method for this problem is the scheme which uses the first algorithm for the wave speeds. It has a sharp shock and models the smooth zone reasonably well. Again the smooth zone in these methods is not modelled nearly as well as it was using (d) and (e). The third algorithm was the worst of the three producing a blunter shock.

i) HLLC SCHEME WITH THE SUPERBEE LIMITER APPLIED TO THE CONTACT FIELD AND MINMOD APPLIED ELSEWHERE.

This is implemented in a similar way to the method shown above for the flux limited HLL scheme.

RESULTS FOR TEST ONE

HLLC with the superbee limiter applied to the contact field, minmod applied elsewhere and using the first algorithm for the wave speeds:

This has a sharp, narrow shock and models the smooth zone well.

HLLC with the superbee limiter applied to the contact field, minmod applied elsewhere and using the second algorithm for the wave speeds :

This is one of our best methods. It has a sharp, narrow shock and models the smooth zone well.

When we apply this method to uniform initial values and look at the results after 30,000 time steps we see that our values have started blowing up.

HLLC with the superbee limiter applied to the contact field, minmod applied elsewhere and using the third algorithm for the wave speeds :

This has a narrow, reasonably sharp shock and models the smooth zone well.

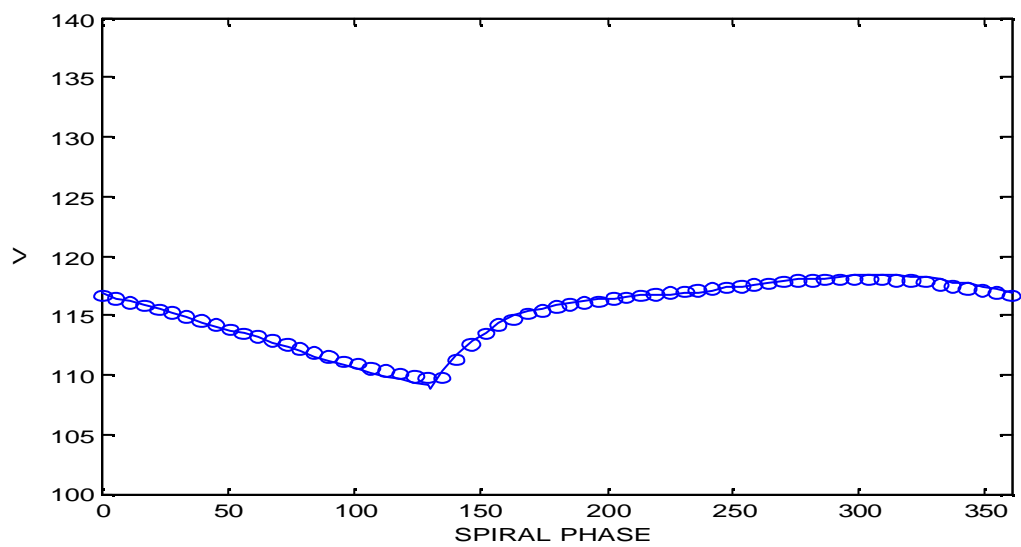
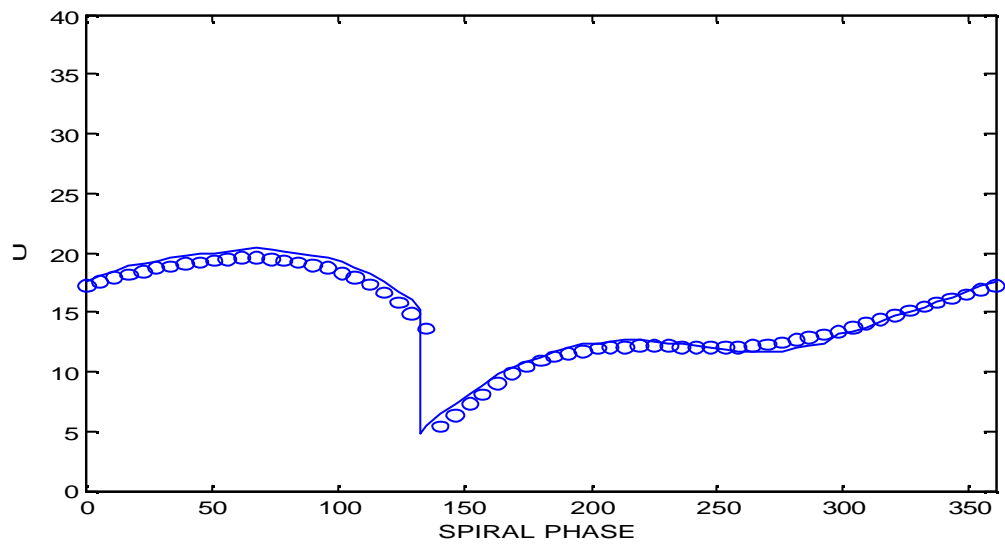
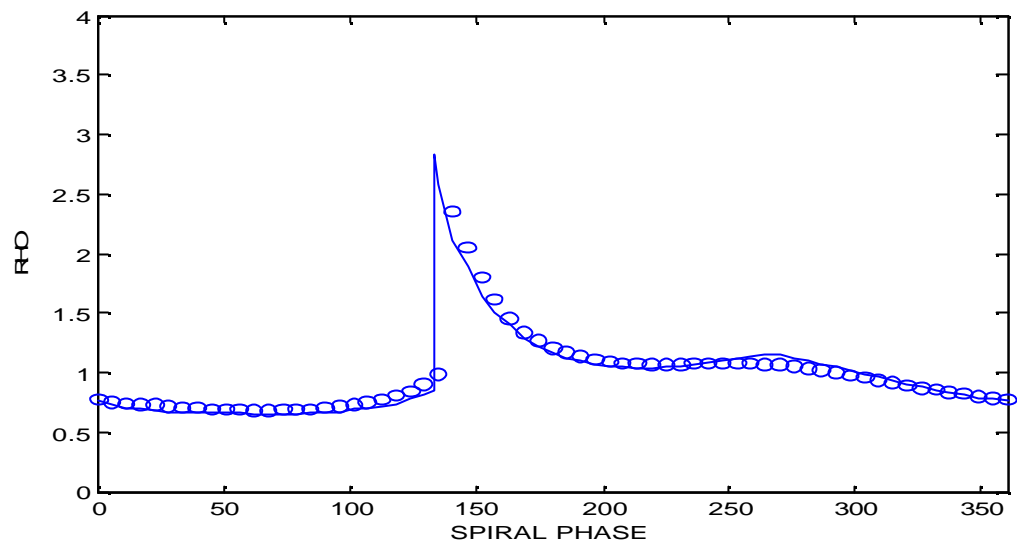
Figure seventeen: Results from the HLLC Scheme with wave speed algorithm (1)

Figure eighteen: Results from the HLLC Scheme with the superbee limiter applied to the contact field, minmod applied elsewhere and using wave speed algorithm (1)

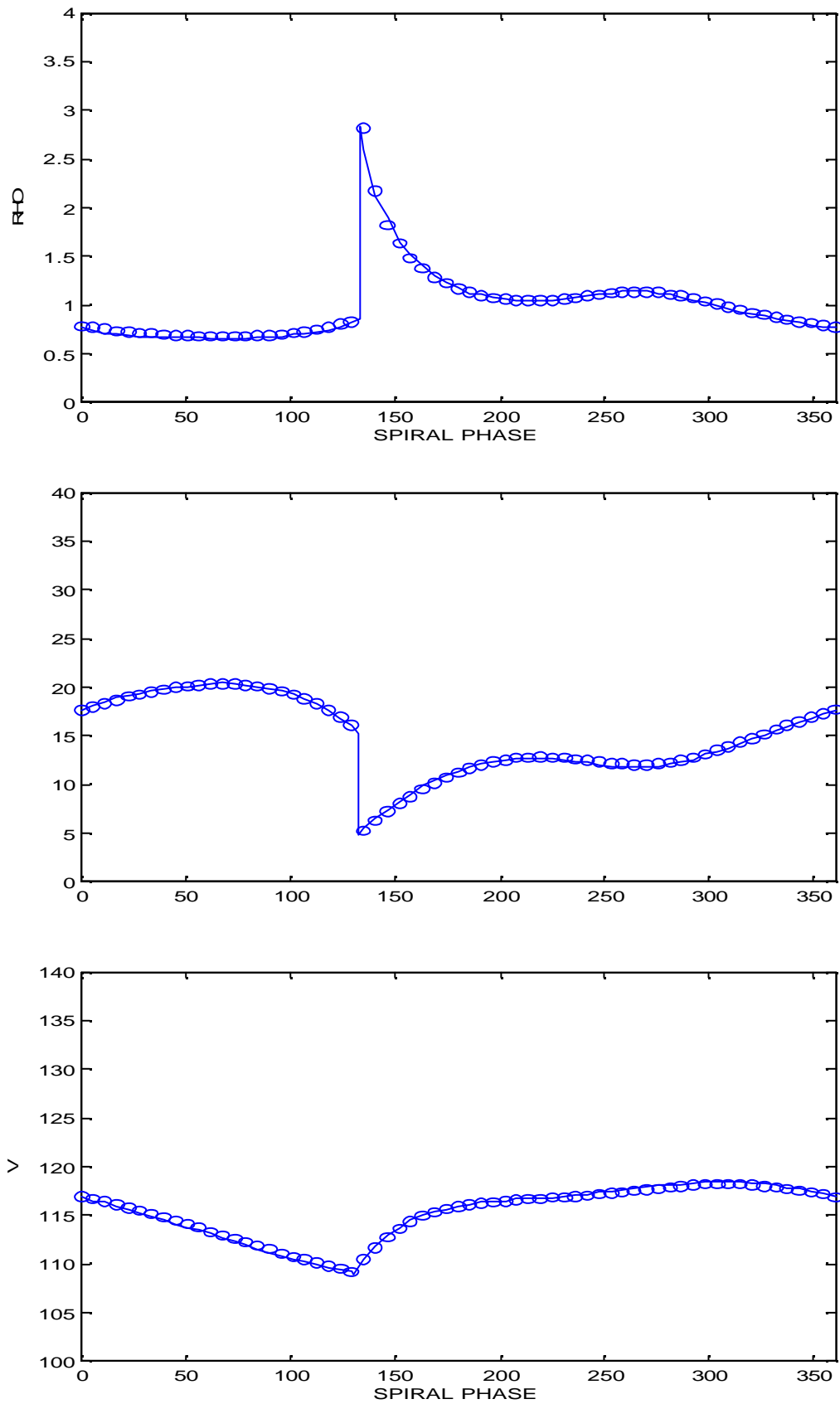


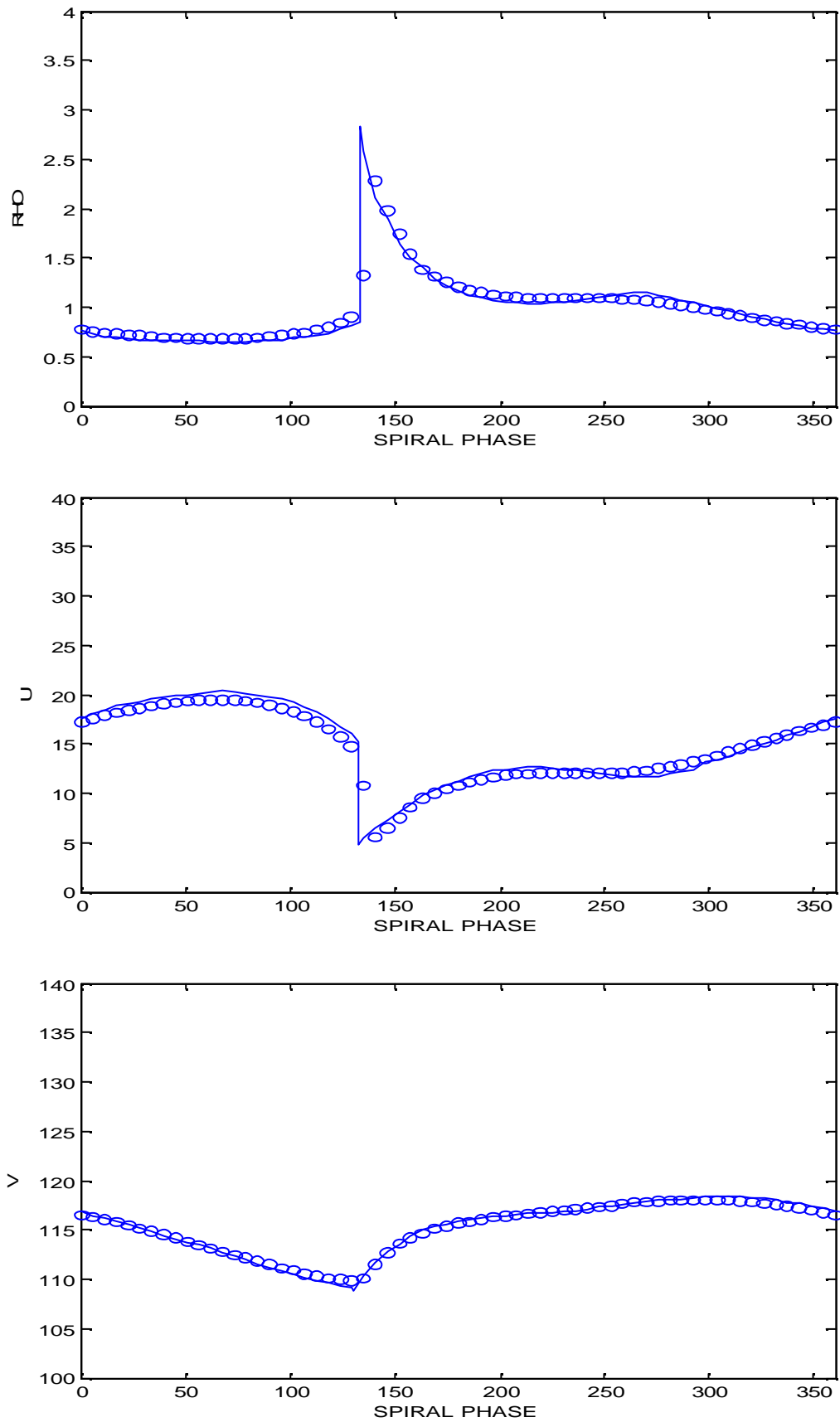
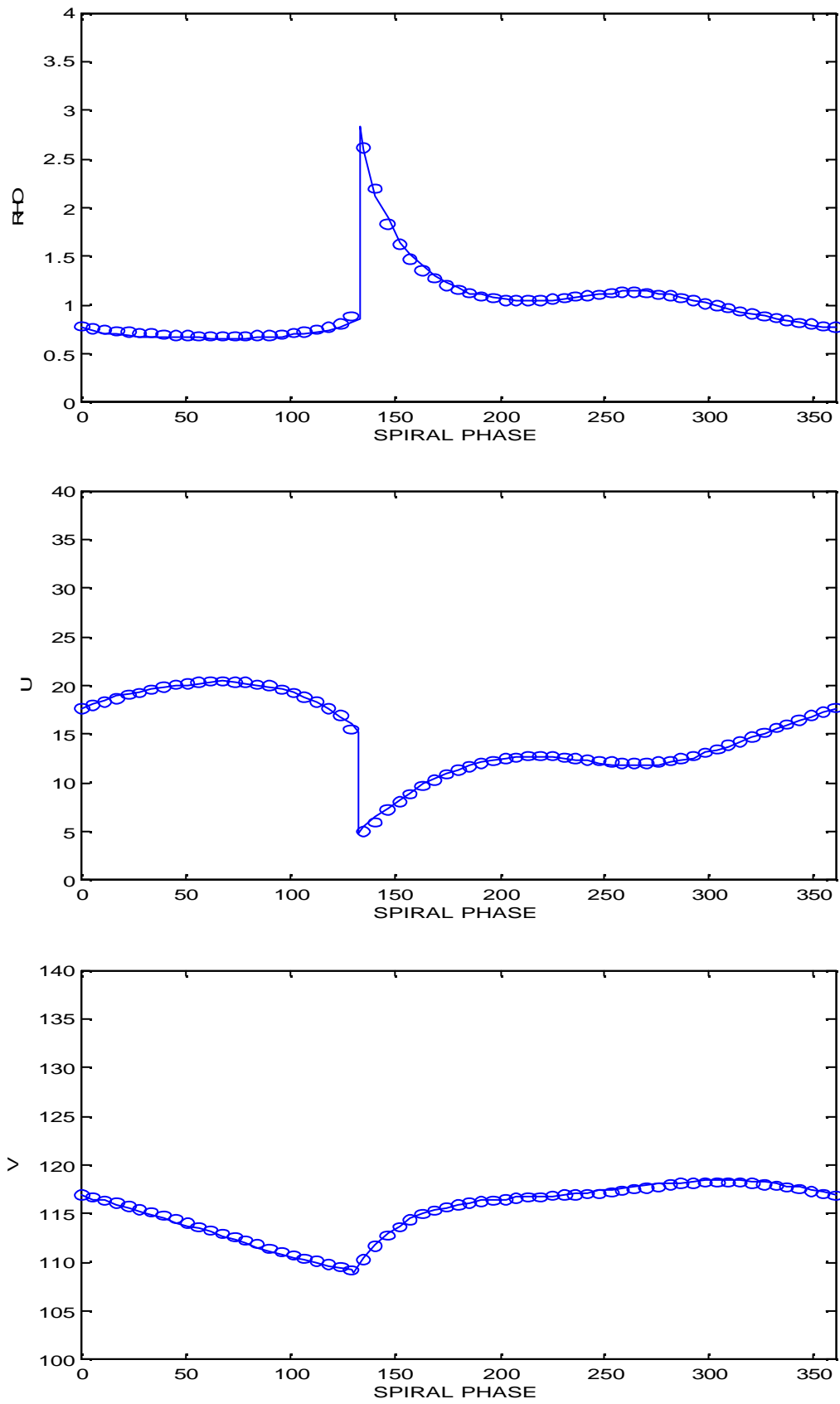
Figure nineteen: Results from the HLLC Scheme with wave speed algorithm (2)

Figure twenty: Results from the HLLC Scheme with the superbee limiter applied to the contact field, minmod applied elsewhere and using wave speed algorithm (2)



After 30,000 time steps using uniform initial values

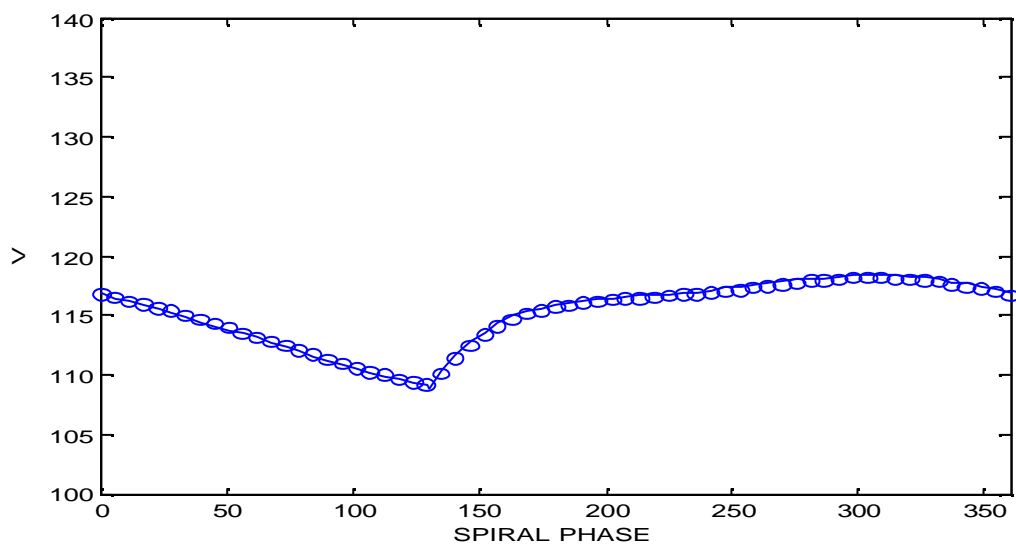
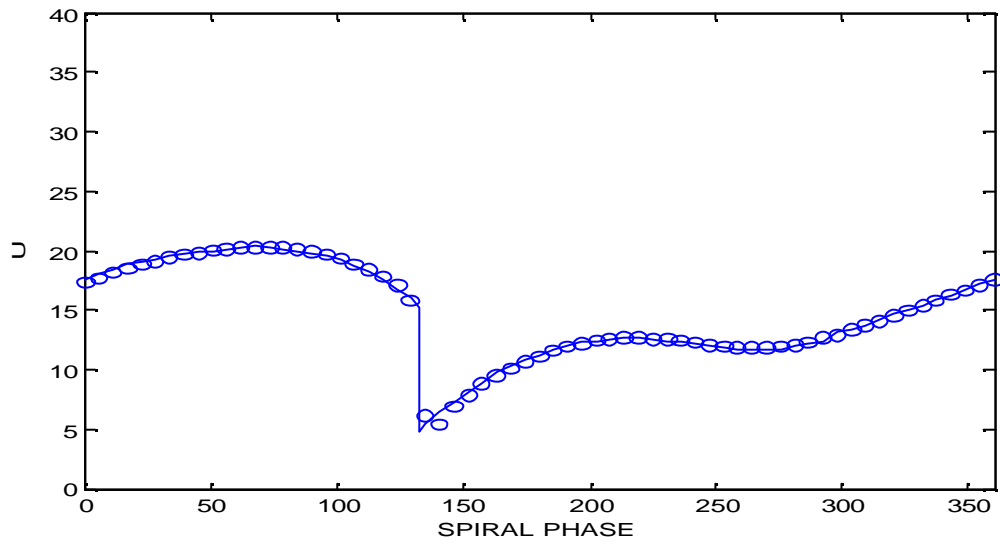
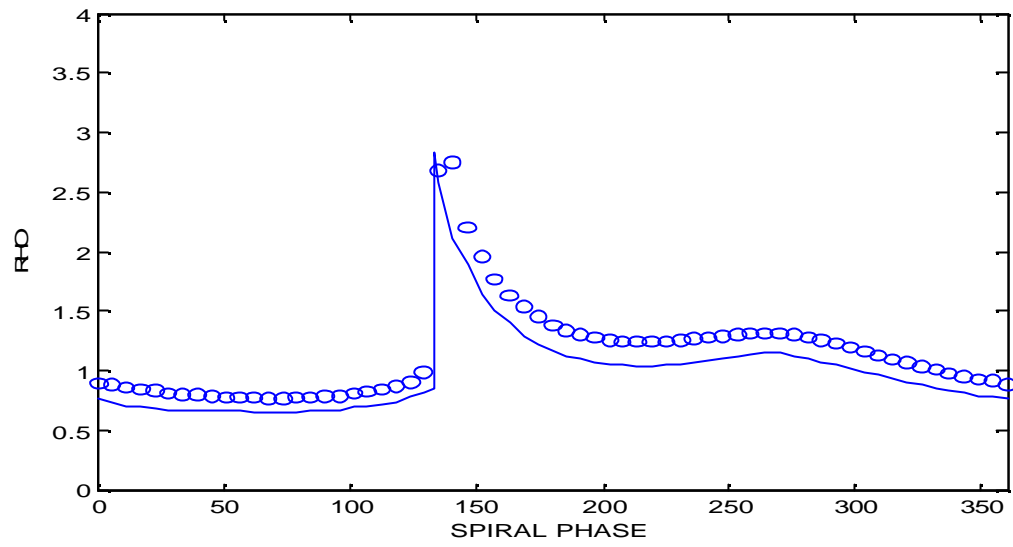


Figure twenty-one: Results from the HLLC Scheme with wave speed algorithm (3)

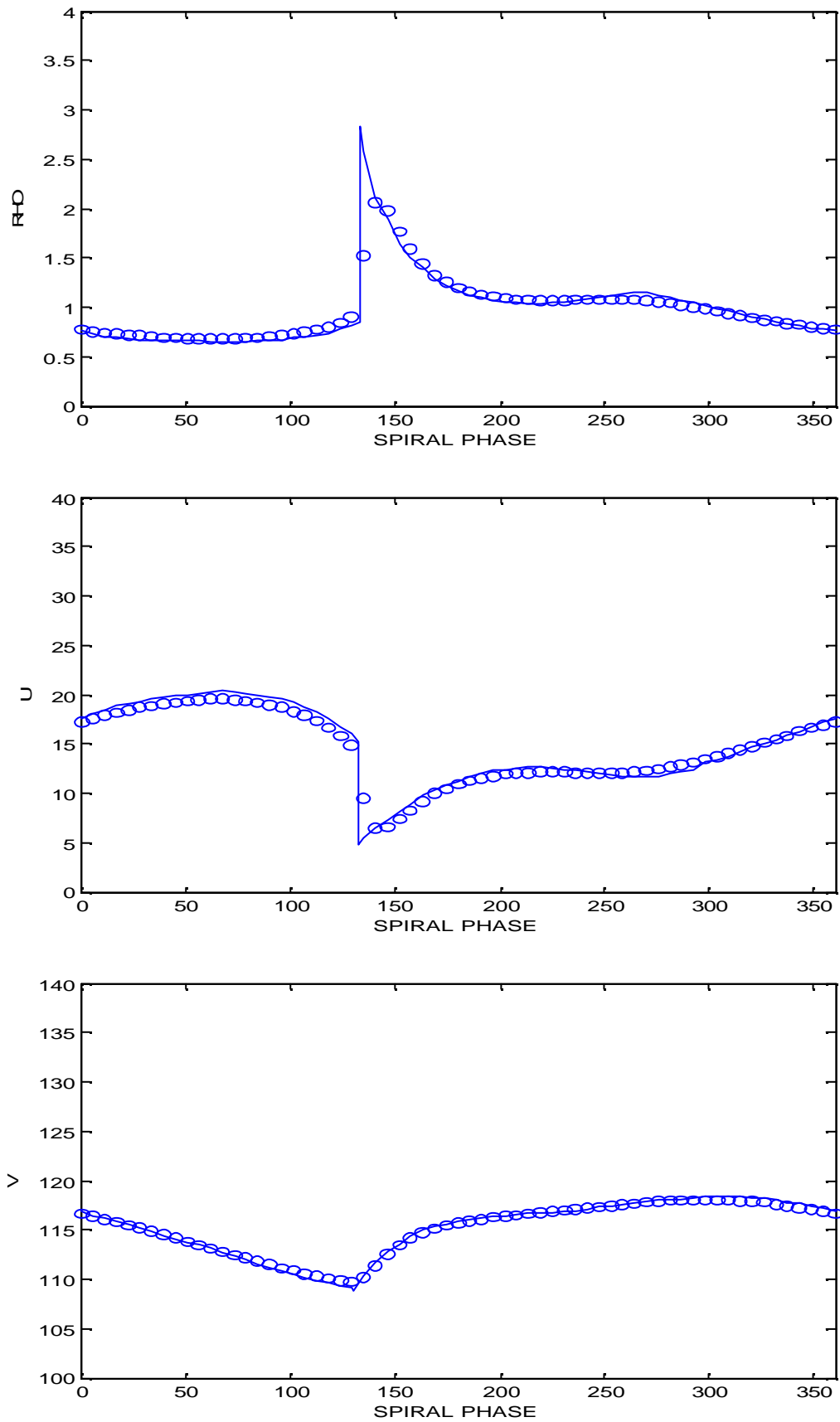
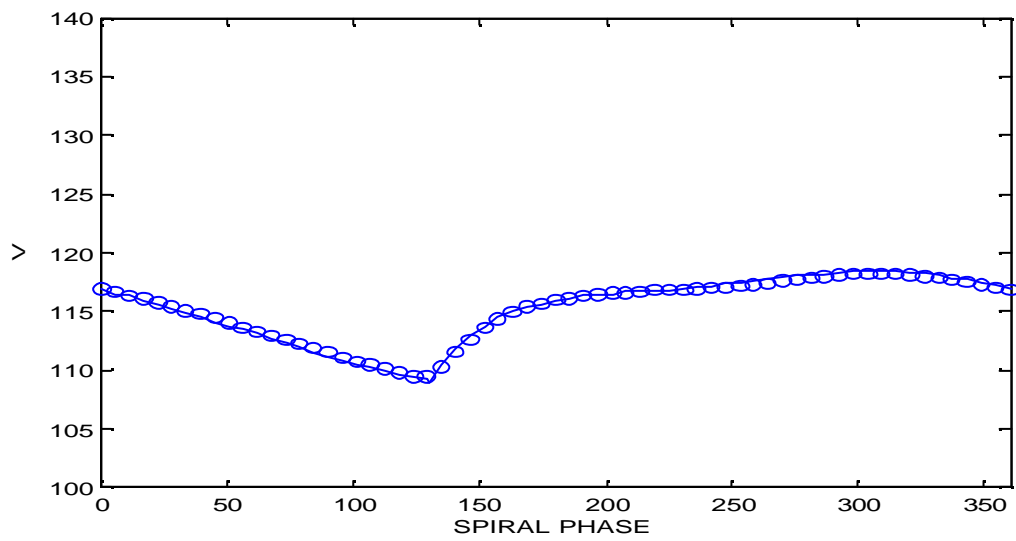
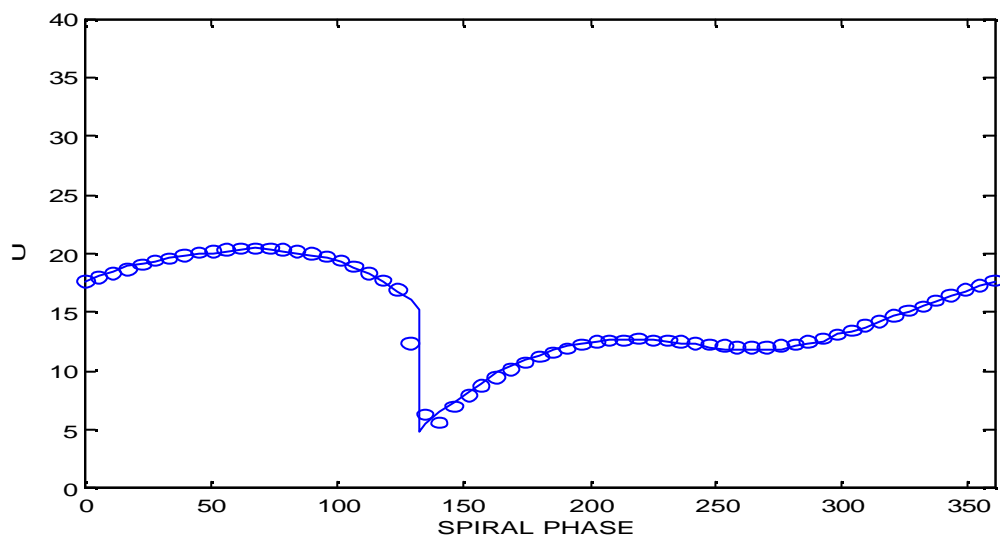
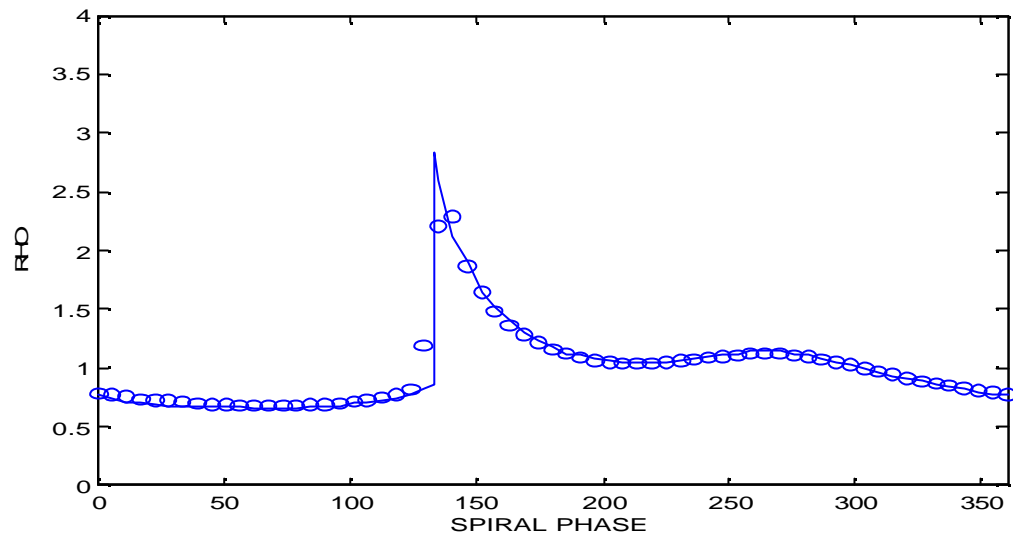


Figure twenty-two: Results from the HLLC Scheme with the superbee limiter applied to the contact field, minmod applied elsewhere and using wave speed algorithm (3)



CALCULATED ERRORS IN THE SMOOTH ZONE

TEST ONE

SCHEME	AVE.OF ABS. ERRORS IN RHO	AVE.OF ABS. ERRORS IN U	AVE.OF ABS. ERRORS IN V
MacCormack's method	0.02213081	0.246966	0.164614
Second-order flux-splitting method	0.0351086	0.53583	0.20800
Roe's method	0.03775312	0.611001	0.230072
Roe's method with minmod limiter	0.02204784	0.198943	0.193965
Roe's method with MC limiter	0.01868166	0.137541	0.186092
Roe's method with van Leer limiter	0.01983648	0.150512	0.189726
Roe's method with minmod and van Leer	0.02064359	0.162159	0.185261
Roe's method with minmod and superbee	0.01729878	0.121218	0.182321
With source term decomposed			
Roe's method	0.01308100	0.149290	0.200135
Roe's method with minmod applied	0.01877022	0.197524	0.148464
Roe's method with MC-limiter applied	0.01759703	0.159043	0.151072
Roe's method with van leer limiter applied	0.01826681	0.156895	0.146105
Roe's method with minmod and van leer	0.01857917	0.169565	0.141185
Roe's method with minmod and superbee	0.01613746	0.157628	0.147561
HLL method (1)	0.03832700	0.528293	0.215260
HLL method (1) with minmod applied	0.03394140	0.328469	0.225486
HLLC method (1)	0.03596082	0.504485	0.206247
HLLC method (1) with minmod and superbee	0.01602880	0.117367	0.193181
HLL method (2)	0.03888338	0.574836	0.229622
HLL method (2) with minmod applied	0.02710122	0.299554	0.208508
HLLC method (2)	0.03569156	0.560873	0.217723
HLLC method (2) with minmod and superbee	0.01631037	0.113876	0.183057
HLL method (3)	0.03622968	0.531410	0.213227
HLL method (3) with minmod applied	0.02913047	0.336032	0.217052
HLLC method (3)	0.03346389	0.504332	0.202928
HLLC method (3) with minmod and superbee	0.01705845	0.125504	0.186109

TEST TWO

SCHEME	AVE.OF ABS. ERRORS IN RHO	AVE.OF ABS. ERRORS IN U	AVE.OF ABS. ERRORS IN V
HLLC method (2) with minmod and superbee	0.171665	4.28341	2.34807
Roe's method with MC limiter	0.174213	4.10867	2.32001
Roe's method with minmod and superbee	0.175255	4.15482	2.37474
With source term decomposed			
Roe's method with minmod applied	0.170250	4.14017	2.28312

RESULTS

In the HLL method the density peak is displaced downstream and only the most general features of the smooth zone are represented. The third algorithm for the signal velocities produced the best results with a density peak that is better represented and a narrower shock. The HLLC scheme is similarly quite poor at modelling the smooth zone. In the first two algorithms it produces sharper shocks than HLL (this is not so for the third). The best algorithm of the three for modelling the shock using the HLLC method is the first one.

The HLL method with the minmod limiter applied improved on the shocks found by the HLL scheme without the limiter but the smooth zone was still not as accurate as we would like. However when we went on to apply a combination of the superbee and minmod limiters to the HLLC scheme we found very good results. The results were particularly good for the schemes which used wave speed algorithms (1) and (2).

Roe's method produces results that are much like the best of the HLL scheme without limiters applied. However these results are substantially improved when we apply the flux limiters to Roe's method. From the limited schemes we find results that follow the smooth zone closely and produce sharper and narrower shocks. All of the plotted limiters showed very good results. The best two are the scheme limited by a combination of the minmod and superbee limiters and that using the MC-limiter. These were closely followed in accuracy by the scheme which was limited by a combination of the minmod and Van Leer limiters.

When we decompose the source term and apply the flux limiters we find similarly good results as for the limited schemes mentioned above. There are a few differences between the two however which is mainly shown in the shock. The shock using the minmod limiter becomes sharper using this method whereas the shock in the scheme using the MC-limiter and the scheme using a combination of the superbee and minmod limiters becomes blunter.

All of our new results produced sharper and narrower shocks than MacCormack's. Roe's scheme with limiters applied, the HLLC scheme with limiter applied, and Roe's method with the source term decomposed and limiters applied produced the best results. They produced good approximations of the smooth zone and modelled the shock well.

The methods that we chose to perform test two on were

- 1) Roe's scheme with the MC limiter applied,
- 2) Roe's scheme with a combination of the minmod and superbee limiters applied,
- 3) Roe's scheme with the source term decomposed and minmod limiter applied,
- 4) The HLLC scheme with a combination of the minmod and superbee limiters applied.

All of the schemes produced similar results in the test. However when we looked at their progression after 30,000 time steps we saw that the results of (1), (2) and (4) blew up whereas (3) stayed close to the exact solution.

CONCLUSIONS AND RECOMMENDATIONS

The programming effort of Roe's scheme with flux limiters applied, the HLLC scheme with flux limiter applied, and Roe's scheme with the source term decomposed and flux limiters applied is similar to that of the second order flux splitting method but the limited schemes produced the better results.

While MacCormack's method and the second order flux splitting method are reasonably accurate in the smooth region of the flow they cannot compare with the best methods found in this study at modelling the shock.

Now, taking the progression after 30,000 time steps into consideration we would prefer Roe's method with the source term decomposed and flux limiters applied out of our preferred methods.

Concisely, we would recommend Roe's scheme with the source term decomposed and flux limiters (in particular minmod) applied to be used in the flow problem.

APPENDIX

In this appendix we show the calculations which enable us to implement our methods.

First, we show the calculations which led to the necessary equations for $\left(\frac{\partial Q}{\partial t}\right)_i^n$ in the

Second order flux splitting method.

Following this are our calculations to find the decomposition and Roe averages used in the Roe scheme.

SECOND-ORDER FLUX-SPLITTING METHOD

The following calculations show how to obtain $\left(\frac{\partial Q}{\partial t}\right)_i^n$ from our calculated values for

$$\left(\frac{\partial Q}{\partial \mathbf{h}}\right)_i^n.$$

Directly from our system of equations we have that:

- i) $\frac{\partial Q}{\partial t} + \frac{\partial(Qu)}{\partial \mathbf{h}} = 0,$
- ii) $\frac{\partial(Qu)}{\partial t} + \frac{\partial(Q(u^2 + c^2))}{\partial \mathbf{h}} = 2\Omega(v - v_0)Q + \frac{2}{\mathbf{ar}}QA \sin \hat{\mathbf{h}},$
- iii) $\frac{\partial(Qv)}{\partial t} + \frac{\partial(Quv)}{\partial \mathbf{h}} = \frac{-k^2}{2\Omega}(u - u_0)Q.$

We can also write (ii) in the following form:

$$\text{iv) } Q \frac{\partial u}{\partial t} + u \frac{\partial Q}{\partial t} + \frac{\partial(Q(u^2 + c^2))}{\partial \mathbf{h}} = 2\Omega(v - v_0)Q + \frac{2}{\mathbf{ar}}QA \sin \hat{\mathbf{h}}.$$

From (iv) minus u multiplied by (i) we obtain

$$Q \frac{\partial u}{\partial t} + \frac{\partial(Q(u^2 + c^2))}{\partial \mathbf{h}} - u \frac{\partial(Qu)}{\partial \mathbf{h}} = 2\Omega(v - v_0)Q + \frac{2}{ar}QA \sin \mathbf{h}.$$

We can now manipulate this equation as shown below:

$$Q \frac{\partial u}{\partial t} + Qu \frac{\partial u}{\partial \mathbf{h}} + u \frac{\partial(Qu)}{\partial \mathbf{h}} + c^2 \frac{\partial Q}{\partial \mathbf{h}} - u \frac{\partial(Qu)}{\partial \mathbf{h}} = 2\Omega(v - v_0)Q + \frac{2}{ar}QA \sin \mathbf{h}$$

which becomes

$$Q \frac{\partial u}{\partial t} + Qu \frac{\partial u}{\partial \mathbf{h}} + c^2 \frac{\partial Q}{\partial \mathbf{h}} = 2\Omega(v - v_0)Q + \frac{2}{ar}QA \sin \mathbf{h}.$$

Therefore we have that

$$\frac{\partial u}{\partial t} = 2\Omega(v - v_0) + \frac{2}{ar}A \sin \mathbf{h} - u \frac{\partial u}{\partial \mathbf{h}} - \frac{c^2}{Q} \frac{\partial Q}{\partial \mathbf{h}}.$$

From (i) by simple manipulation we find

$$\frac{\partial Q}{\partial t} = \frac{-\partial(Qu)}{\partial \mathbf{h}} = (-Q) \frac{\partial u}{\partial \mathbf{h}} + (-u) \frac{\partial Q}{\partial \mathbf{h}}.$$

From (iii) we find

$$v \frac{\partial Q}{\partial t} + Q \frac{\partial v}{\partial t} + \frac{\partial(Quv)}{\partial \mathbf{h}} = \frac{-k^2}{2\Omega}(u - u_0)Q.$$

Now, by taking (i) multiplied by v away from this equation we get

$$v \frac{\partial Q}{\partial t} + Q \frac{\partial v}{\partial t} + \frac{\partial(Quv)}{\partial \mathbf{h}} - v \frac{\partial Q}{\partial t} - v \frac{\partial(Qu)}{\partial \mathbf{h}} = \frac{-k^2}{2\Omega}(u - u_0)Q.$$

After some manipulation this becomes

$$Q \frac{\partial v}{\partial t} + (Qu) \frac{\partial v}{\partial \mathbf{h}} + v \frac{\partial(Qu)}{\partial \mathbf{h}} - v \frac{\partial(Qu)}{\partial \mathbf{h}} = \frac{-k^2}{2\Omega}(u - u_0)Q.$$

From which we find

$$\frac{\partial v}{\partial t} = \frac{-k^2}{2\Omega}(u - u_0) - u \frac{\partial v}{\partial \mathbf{h}}.$$

Finally, we have obtained the following equations:

$$\frac{\partial Q}{\partial t} = (-Q) \frac{\partial u}{\partial \mathbf{h}} + (-u) \frac{\partial Q}{\partial \mathbf{h}}.$$

$$\frac{\partial u}{\partial t} = 2\Omega(v - v_0) + \frac{2}{ar} A \sin \mathbf{h} - u \frac{\partial u}{\partial \mathbf{h}} - \frac{c^2}{Q} \frac{\partial Q}{\partial \mathbf{h}}.$$

$$\frac{\partial v}{\partial t} = \frac{-k^2}{2\Omega} (u - u_0) - u \frac{\partial v}{\partial \mathbf{h}}.$$

ROE'S SCHEME

Taking

$$U = \begin{pmatrix} Q \\ Qu \\ Qv \end{pmatrix} = \begin{pmatrix} Q \\ m \\ n \end{pmatrix}.$$

We have

$$F = \begin{pmatrix} Qu \\ Q(u^2 + c^2) \\ Quv \end{pmatrix} = \begin{pmatrix} m \\ \frac{m^2}{Q} + Qc^2 \\ \frac{mn}{Q} \end{pmatrix}.$$

Next, we work out the derivative of F as follows:

$$A = \begin{pmatrix} 0 & 1 & 0 \\ \frac{-m^2}{Q^2} + c^2 & \frac{2m}{Q} & 0 \\ \frac{-mn}{Q^2} & \frac{n}{Q} & \frac{m}{Q} \end{pmatrix} = \begin{pmatrix} 0 & 1 & 0 \\ c^2 - u^2 & 2u & 0 \\ -uv & v & u \end{pmatrix}.$$

We now go on to find the eigenvalues and eigenvectors of this matrix.

FINDING OUR EIGENVALUES

$$\det(A - \mathbf{I}I) = 0$$

$$\begin{vmatrix} -\mathbf{I} & 1 & 0 \\ c^2 - u^2 & 2u - \mathbf{I} & 0 \\ -uv & v & u - \mathbf{I} \end{vmatrix} = (-\mathbf{I})[(2u - \mathbf{I})(u - \mathbf{I}) - 0] - [(c^2 - u^2)(u - \mathbf{I}) - 0] + 0$$

$$= (-\mathbf{I})(2u - \mathbf{I})(u - \mathbf{I}) - (c^2 - u^2)(u - \mathbf{I})$$

$$= -\mathbf{I}^3 + 3u\mathbf{I}^2 + (c^2 - 3u^2)\mathbf{I} + (u^3 - c^2u)$$

$$= -(\mathbf{I} - u)(\mathbf{I} - (u + c))(\mathbf{I} - (u - c)) = 0.$$

Therefore our eigenvalues are u , $u + c$, $u - c$.

FINDING OUR EIGENVECTORS

$$A\underline{r} = \mathbf{I}\underline{r}$$

$$(i) \begin{pmatrix} 0 & 1 & 0 \\ c^2 - u^2 & 2u & 0 \\ -uv & v & u \end{pmatrix} \begin{pmatrix} x \\ y \\ z \end{pmatrix} = u \begin{pmatrix} x \\ y \\ z \end{pmatrix}$$

from which we have

$$y = ux,$$

$$(c^2 - u^2)x + 2uy = uy,$$

$$-(uv)x + vy + uz = uz.$$

From the first of the three equations we find

$$x = \frac{y}{u},$$

and substituting this into the second equation we have

$$(c^2 - u^2)\frac{y}{u} + 2uy = uy.$$

By manipulating this equation we find

$$c^2y = 0 \text{ and so } y = 0.$$

Therefore by the above equation we must have that

$$x = 0.$$

Now, substituting these values into the third equation we find that our z can be any

value. One of our eigenvectors is therefore $\begin{pmatrix} 0 \\ 0 \\ 1 \end{pmatrix}$.

$$(ii) \begin{pmatrix} 0 & 1 & 0 \\ c^2 - u^2 & 2u & 0 \\ -uv & v & u \end{pmatrix} \begin{pmatrix} x \\ y \\ z \end{pmatrix} = (u + c) \begin{pmatrix} x \\ y \\ z \end{pmatrix},$$

from which we have

$$y = (u + c)x,$$

$$(c^2 - u^2)x + 2uy = (u + c)y,$$

$$-uvx + vy + uz = (u + c)z.$$

From the first of the three equations we find

$$x = \frac{y}{u + c},$$

and by substituting this into the second equation we have

$$\frac{(c^2 - u^2)y}{u + c} + 2uy = (u + c)y.$$

By manipulating this equation we find

$$y = y.$$

Now, if we take

$$x = 1,$$

$$y = u + c,$$

and substitute these values into the third equation we find

$$-uv + v(u + c) + uz = (u + c)z$$

from which we have

$$cz = cv \text{ and so that } z = v.$$

The second of our eigenvectors is therefore $\begin{pmatrix} 1 \\ u + c \\ v \end{pmatrix}$.

$$(iii) \begin{pmatrix} 0 & 1 & 0 \\ c^2 - u^2 & 2u & 0 \\ -uv & v & u \end{pmatrix} \begin{pmatrix} x \\ y \\ z \end{pmatrix} = (u - c) \begin{pmatrix} x \\ y \\ z \end{pmatrix},$$

from which we have

$$y = (u - c)x,$$

$$(c^2 - u^2)x + 2uy = (u - c)y,$$

$$-uvx + vy + uz = (u - c)z.$$

From the first of the three equations we find

$$x = \frac{y}{u - c},$$

and substituting this into the second equation we have

$$\frac{(c^2 - u^2)y}{u - c} + 2uy = (u - c)y .$$

By manipulating this equation we find

$$y = y .$$

Now, if we take

$$x = 1 ,$$

$$y = u - c ,$$

and substitute these values into the third equation we find

$$-uv + v(u - c) + uz = (u - c)z$$

from which we have

$$-cv = -cz \text{ and so that } z = v .$$

Our third eigenvector is therefore $\begin{pmatrix} 1 \\ u - c \\ v \end{pmatrix}$.

Finally, we have found that our three right eigenvectors are as follows:

$$\begin{pmatrix} 0 \\ 0 \\ z \end{pmatrix}, \begin{pmatrix} 1 \\ u + c \\ v \end{pmatrix} \text{ and } \begin{pmatrix} 1 \\ u - c \\ v \end{pmatrix} .$$

We can now find our left eigenvectors by finding the inverse of the following matrix.

$$\begin{pmatrix} 1 & 1 & 0 \\ u + c & u - c & 0 \\ v & v & 1 \end{pmatrix} .$$

Finding the inverse:

$$\begin{aligned}
& \left(\begin{array}{ccc|ccc} 1 & 1 & 0 & 1 & 0 & 0 \\ u+c & u-c & 0 & 0 & 1 & 0 \\ v & v & 1 & 0 & 0 & 1 \end{array} \right) \begin{array}{l} (i) \\ (ii) \\ (iii) \end{array} \\
& = \left(\begin{array}{ccc|ccc} 1 & 1 & 0 & 1 & 0 & 0 \\ u+c & u-c & 0 & 0 & 1 & 0 \\ 0 & 0 & 1 & -v & 0 & 1 \end{array} \right) \begin{array}{l} (i) \\ (ii) \\ (iv) = (iii) - v(i) \end{array} \\
& = \left(\begin{array}{ccc|ccc} 1 & 1 & 0 & 1 & 0 & 0 \\ 0 & -2c & 0 & -(u+c) & 1 & 0 \\ 0 & 0 & 1 & -v & 0 & 1 \end{array} \right) \begin{array}{l} (i) \\ (v) = (ii) - (u+c)(i) \\ (iv) \end{array} \\
& = \left(\begin{array}{ccc|ccc} 1 & 0 & 0 & 1 - \frac{(u+c)}{2c} & \frac{1}{2c} & 0 \\ 0 & -2c & 0 & -(u+c) & 1 & 0 \\ 0 & 0 & 1 & -v & 0 & 1 \end{array} \right) \begin{array}{l} (vi) = (i) - \frac{1}{2c}(v) \\ (v) \\ (iv) \end{array} \\
& = \left(\begin{array}{ccc|ccc} 1 & 0 & 0 & \frac{(c-u)}{2c} & \frac{1}{2c} & 0 \\ 0 & 1 & 0 & \frac{(u+c)}{2c} & \frac{-1}{2c} & 0 \\ 0 & 0 & 1 & -v & 0 & 1 \end{array} \right) \begin{array}{l} (vi) \\ (vii) = \frac{-1}{2c}(v) \\ (iv) \end{array}
\end{aligned}$$

Therefore our inverse is as follows:

$$\frac{1}{2c} \begin{pmatrix} (c-u) & 1 & 0 \\ (u+c) & -1 & 0 \\ -2cv & 0 & 2c \end{pmatrix}$$

and so our left eigenvectors are

$$\begin{pmatrix} \frac{(c-u)}{2c} \\ \frac{1}{2c} \\ 0 \end{pmatrix}, \begin{pmatrix} \frac{(u+c)}{2c} \\ \frac{-1}{2c} \\ 0 \end{pmatrix} \text{ and } \begin{pmatrix} -v \\ 0 \\ 1 \end{pmatrix}.$$

ROE AVERAGES

As a parameter vector we choose

$$\underline{z} = \sqrt{Q} \begin{pmatrix} 1 \\ u \\ v \end{pmatrix},$$

from which we find

$$u = \begin{pmatrix} Q \\ Qu \\ Qv \end{pmatrix} = \begin{pmatrix} (z_1)^2 \\ z_1 z_2 \\ z_1 z_3 \end{pmatrix},$$

$$\frac{\partial u}{\partial z} = \begin{pmatrix} 2z_1 & 0 & 0 \\ z_2 & z_1 & 0 \\ z_3 & 0 & z_1 \end{pmatrix},$$

$$F = \begin{pmatrix} Qu \\ Q(u^2 + c^2) \\ Quv \end{pmatrix} = \begin{pmatrix} z_1 z_2 \\ (z_2)^2 + c^2 (z_1)^2 \\ z_2 z_3 \end{pmatrix},$$

$$\frac{\partial F}{\partial z} = \begin{pmatrix} z_2 & z_1 & 0 \\ 2c^2 z_1 & 2z_2 & 0 \\ 0 & z_3 & z_2 \end{pmatrix},$$

and

$$\bar{A}(u_L, u_R) = \begin{pmatrix} 0 & 1 & 0 \\ c^2 - \bar{u}^2 & 2\bar{u} & 0 \\ -\bar{u}\bar{v} & \bar{v} & \bar{u} \end{pmatrix} \text{ where } \bar{u} \text{ and } \bar{v} \text{ are the Roe averages as defined}$$

below:

$$\bar{u} = \frac{\bar{z}_2}{\bar{z}_1} = \frac{\sqrt{Q_R} u_R + \sqrt{Q_L} u_L}{\sqrt{Q_R} + \sqrt{Q_L}},$$

$$\bar{v} = \frac{\bar{z}_3}{\bar{z}_1} = \frac{\sqrt{Q_R} v_R + \sqrt{Q_L} v_L}{\sqrt{Q_R} + \sqrt{Q_L}}.$$

ACKNOWLEDGEMENTS

I would like to thank Dr.P.K.Sweby for all his help. I am also grateful for the financial support received from EPSRC.

REFERENCES

- Bermudez, A., Vazquez, M.: 1994, *Computers Fluids*, Vol.23, No.8, 1049. [1]
- Einfeldt, B.: 1988, *SIAM J. on Numerical Anal.*, Vol.25, Issue 2, 294. [2]
- Leveque, R.J.: *Finite Volume Methods for Hyperbolic Problems*,
Cambridge Texts in Applied Mathematics. [3]
- Leveque, R.J.: *Numerical Methods in Conservation Laws*. [4]
- Lin, C.C., Lau, Y.Y.: 1979, *Studies in Appl. Math.* **60**, 97. [5]
- Lin, C.C., Shu, F.H.: 1964, *Astrophysics J.* **140**, 646. [6]
- Lin, C.C., Shu, F.H.: 1966, *Proc. Natl. Acad. Sci. USA.* **55**, 229. [7]
- Roberts, W.W.: 1969, *Astrophysics J.* **158**, 123. [8]
- Sanders, R.H., Prendergast, K.H.: 1974, *Astrophysics J.* **188**, 489. [9]
- Shu, F.H., Milione, V., Roberts, W.W.: 1973, *Astrophysics J.* **183**, 819. [10]
- Toomre, A.: 1977, *Ann. Rev. Astron. Astrophys.* **15**, 437. [11]
- Van Albada, G.D., Van Leer, B., Roberts, Jr, W.W.: 1982, *Astronomy and
Astrophysics.* **108**, 76. [12]
- Van Leer, B.:1977, *J. Computational Phys.* **23**, 276. [13]
- Van Leer, B.:1981b, ICASE Report. [14]
- Woodward, P.R.:1975, *Astrophysics J.* **195**, 61. [15]